ISSN 1819-7140, Russian Journal of Pacific Geology, 2022, Vol. 16, No. 4, pp. 281–299. © Pleiades Publishing, Ltd., 2022.
Russian Text © The Author(s), 2022, published in Tikhookeanskaya Geologiya, 2022, Vol. 41, No. 4, pp. 3–22.

The Khanka Massif: The Heterogeneity of its Basement and Regional Correlations

A. I. Khanchuk[a, c, *], A. A. Alenicheva[b], V. V. Golozubov[a], A. T. Kandaurov[c], Y. Y. Yurchenko[b], and S. A. Sergeev[b]

[a] *Far East Geological Institute, Far Eastern Branch, Russian Academy of Sciences, Vladivostok, 690022 Russia*
[b] *Russian Geological Research Institute (VSEGEI), St. Petersburg, 199106 Russia*
[c] *Novosibirsk State University, Novosibirsk, 630090 Russia*
**e-mail: axanchuk@mail.ru*

Received December 17, 2021; revised January 10, 2022; accepted March 16, 2022

Abstract—This paper reports new geochronological data on metagranitoids (U–Pb SIMS) and ophiolites (Sm–Nd) from the Khanka massif. New and published data define the Early Neoproterozoic Matveevka–Nakhimovka terrane with 935- and 915-Ma early suprasubduction magmatism, 850–880-Ma and 757-Ma withinplate and Pacific-type transform margin magmatism, as well as the Late Neoproterozoic–Early Cambrian Dvoryan and Tafuin terranes with 543, 520, 517, and 513-Ma suprasubduction magmatism. These two terranes are separated by a suture (Voznesenka and Spassk terranes) formed by Ediacaran–Cambrian shelf deposits and a Cambrian accretionary wedge with ophiolites older than 514 Ma. The greater part of the Khanka massif formed in the late Cambrian, with the Kordonka island-arc terrane accreted at the end of the Silurian. The Sergeevka terrane of the Ordovician island arc joined it through the Early Cretaceous strike-slip movements. Heterogeneous structures of the main part of the Khanka massif can be traced to the north based on the analogous stages of magmatism and metamorphism, where the Jiamusi massif (including the East Bureya terrane) is an Early Neoproterozoic block and the eastern Songnen massif (including the West Bureya terrane) is a Late Neoproterozoic–Cambrian block. These blocks are separated by the Spassk–Wuxingzhen–Melgin suture formed by their collision in the Late Cambrian. The Bureya–Songnen–Jiamusi–Khanka superterrane formed as a part of the Gondwana supercontinent approximately 500 Ma ago through orogeny and accretion of the Rodinia supercontinent fragments.

Keywords: Neoproterozoic, Cambrian, geochronology, granites, ophiolites, Khanka massif, Bureya–Songnen–Jiamusi–Khanka superterrane

DOI: 10.1134/S1819714022040042

INTRODUCTION

Phanerozoic orogenic belts and Precambrian continental blocks (massifs) are distinguished between the Siberian (in the north) and Sino-Korean (in the south) cratons. Orogenic belts represent continental crust (lithosphere) that was formed on the site of and (or) on the margin of the former oceanic basin owing to the terrane accretion to continents (craton) or during collision of continental blocks. A collage of several massifs or blocks is distinguished in the eastern part of the southern Russian Far East and adjacent areas of China. It is surrounded by Paleozoic and Mesozoic orogenic belts, whose basement is made up of Precambrian and Cambrian complexes: Songnen (Songliao, Bureya, Jiamusi, and Khanka). These massifs are separated by late faults, have similar geological structures, and are considered as the Manchurides [78], Bureya–Jiamusi superterrane [28, 74], and Bureya–Jiamusi paleoplate [62], below called the Bureya–Songnen–Jiamusi–Khanka (BSJK) superterrane. The BSJK superterrane is also considered as being ascribed to the eastern part of the Central Asian Orogenic Belt [8, 42, 57, 64, 66–69, 91, 95–98, 102, 103, and others].

The BSJK superterrane (Fig. 1) from the east and north is in contact with the Late Albian–Cenomanian Sikhote-Alin [47] and Middle Jurassic Mongolian–Okhotsk [82] orogenic belts. In the northeast, the BSJK superterrane borders the South Mongolian–Xing'an [28] or Xing'an [66] belt, which is made up of the pre-Late Carboniferous Paleozoic subduction–accretion complex devoid of Precambrian basement [32, 33, 55, 56, 64, 65, and others]. In the south and southeast, the BSJK superterrane borders the orogenic belt, which was formed through a scissor-like closure of the Solonker ocean at the end of Permian–Middle Triassic from the west eastward [54, 64, 70, 79, and others].

Some believe that the exposures of the Jurassic Heilongjiang accretionary complex mark a Jurassic

Fig. 1. Pre-Mesozoic complexes of the Khanka massif and adjacent areas (inset shows the structural units of the basement of the East Asian continental part, modified according to [5, 28, 73]. Using data [3, 6, 14–20, 28, 29, 44, 45, 49-52, 59, 74, 75, 79, 85, 86, 88, 89, 91, 94-98, 100, 101]. (*1*) undivided Mesozoic and Cenozoic complexes; (*2*) a fragment of the Middle–Late Jurassic accretionary wedge; (*3*) Early–Middle Triassic metamorphic complex with mainly Permian age of protolith; (*4*) Permian terrigenous shelf deposits and limestones; (*5*) Permian basic–felsic volcanic rocks, shallow-marine tuffaceous–terrigenous deposits and limestones; (*6*) Early Carboniferous continental rhyolites and dacites; (*7*) Devonian continental basic–felsic volcanic rocks and their tuffs, more rarely, shallow marine deposits; (*8*) Early Silurian island-arc basalts, andesites, and sedimentary deposits (Kordonka Formation); (*9*) Late Ordovician (~470–455 Ma) continental rhyolites and tuffs; (*10*) Cambrian–Ediacaran shelf and accretionary complexes with Ediacaran–Early Cambrian paleooceanic rock; (*11*) Neoproterozoic (a) and Late Neoproterozoic–Early Cambrian (b) volcanogenic–sedimentary complexes zonally metamorphosed in the greenschist–granulite facies conditions at the end of Cambrian; (*12*) Permian granitoids; (*13*) Late Permian–Early Triassic (?) Ural–Alaskan-type peridotites and gabbros; (*14*) Early Carboniferous leucogranites; (*15*) Early Devonian granites (420–409 Ma); (*16*) Silurian (432–422 Ma) granitoids; (*17*) Late Ordovician (~460–450 Ma) granitoids; (*18*) Middle Ordovician granites (Taudemin Complex) (~475–460 Ma); (*19*) Early Ordovician gabbros, diorites, and granodiorite gneisses (Sergeevka complex); (*20*) Late Cambrian–Early Ordovician granitoids (502–479 Ma); (*21*) Early Cambrian gabbros (a) and granitoids (b); (*22*) Neoproterozoic granitoids, rarely basic rocks; (*23*) ophiolites; (*24*) Early Cretaceous sinistral strike-slip; (*25*) tectonic boundary; (*26*) outlines of tectonic windows of the Heilongjiang complex or remnants of the Sergeevka terrane. Terranes: (DV) Dvoryan; (GR) Grodekovo; (JM) Jiamusi; (KB) Kabarga; (KR) Kordonka; (MN) Matveevka–Nakhimovka; (SR) Sergeevka; (SP) Spassk; (TF) Tafuin; (VS) Voznesenka.

suture between the Songnen and Jiamusi massifs [91, 92, 101, and others]. However, the isolation of exposures of the Heilongjiang Complex and an intricate paleotectonic reconstructions of the NS-trending Triassic ocean with no continuation to the south and north seem to be ambiguous. The Heilongjiang Complex can be considered as the continuation of the Jurassic continental-margin accretionary complex of Sikhote Alin (model of gentle subduction) exhumed at the terminal Early Cretaceous [7].

The characteristic feature of the BSJK superterrane is the wide development of amphibolite- and locally granulite-facies metamorphic rocks, whose age was initially estimated as Archean and Paleoproterozoic based on their high metamorphic grade. Later, U–Pb* dating of metamorphic zircon from the Jiamusi massif yielded a Late Cambrian age of ~500 Ma for the granulite-facies metamorphism [89, 102] and 506 Ma for granulites from the northern Khanka massif [44].[1] Sm–Nd isotope studies and U–Pb dating of detrital zircon showed that the protoliths of high-grade rocks have Neoproterozoic and Cambrian ages instead of previously inferred Early Precambrian age [12, 13, 23, 27, 44, 67, 69, 81, 87, 91, 96, and others].

Data on magmatism predating ~500-Ma regional metamorphism is of special interest for reconstructing the early geological evolution of the BSJK superterrane. Until recently, the oldest date (757 Ma) was the crystallization age of a basic sill, which is the protolith of two-pyroxene–amphibole schist in the Matveevka Formation of the Khanka massif [44]. However, different stages of Neoproterozoic magmatism were recently determined within the BSJK superterrane: 940–933 and 804–789 Ma [42], 937–933 and 896–891 Ma [98], 898–891 Ma [96], 757–751 Ma [97], 917–911, 841 Ma [68], and 929–927, 895 Ma [69].

In this paper we report geochronological data on the Neoproterozoic and Cambrian granitoids (U–Pb SIMS) and ophiolites (Sm–Nd) of the Khanka massif. Based on obtained and available data, the structural scheme of the Khanka massif was specified and a new scheme of the BSJK superterrane was proposed.

THE GEOLOGICAL STRUCTURE OF THE KHANKA MASSIF

The Khanka massif is distinguished as the distribution area of Precambrian and Cambrian complexes. Its northern boundary is the Early Cretaceous Dunhua–Mishan fault of the Tan Lu Fault zone (Fig. 1). In the east and west, the massifs borders the fragment of the Jurassic accretionary wedge and Permian–Middle Triassic orogenic belt. Its northeastern part comprises Late Precambrian–Cambrian complexes that experienced the early stage low-grade metamorphism (amphibolite and epidote–amphibolite facies) around 730 Ma and late-stage high-grade metamorphism under the greenschist to granulite facies at the end of Cambrian (~506 Ma) [23, 44]. Stratigraphic units were recognized by metamorphic grade and their position in the section is conditional [23]. The granulite–amphibolite complexes are united into the Iman Group (Ruzhinka and Matveevka formations), while amphibolite complexes, into the Ussuri Group including the Nakhimovka, Tat'yanovka, and Turgenevka formations. The epidote–amphibolite–greenschist complex is distinguished as the Lesozavodsk Group (Kabarga, Spassk, and Mitrofanovka formations). Neoproterozoic oncolites were found in the dolomites of the Spassk Formation [3]. The Orlovka Group distinguished in the Kabarga zone is made up of amygdaloidal basalts, limestones, quartzites with manganese ores, schists and sandstones [3]. Amphibolite-facies metamorphic complexes were recently mapped in the western Khanka massif (Kraevskaya and Il'inka formations) [19]. The central part of the massif (Spassk zone with the Evgen'evskaya Group and Voznesenka zone with the Yaroslavka and Grigor'evskaya groups) is made up of the Cambrian terrigenous–carbonate rocks bearing archeocyates from the Fortunian to stage 3 (from the Tommotian to

[1] Further, if not indicated, age dates were obtained by U–Pb zircon dating.

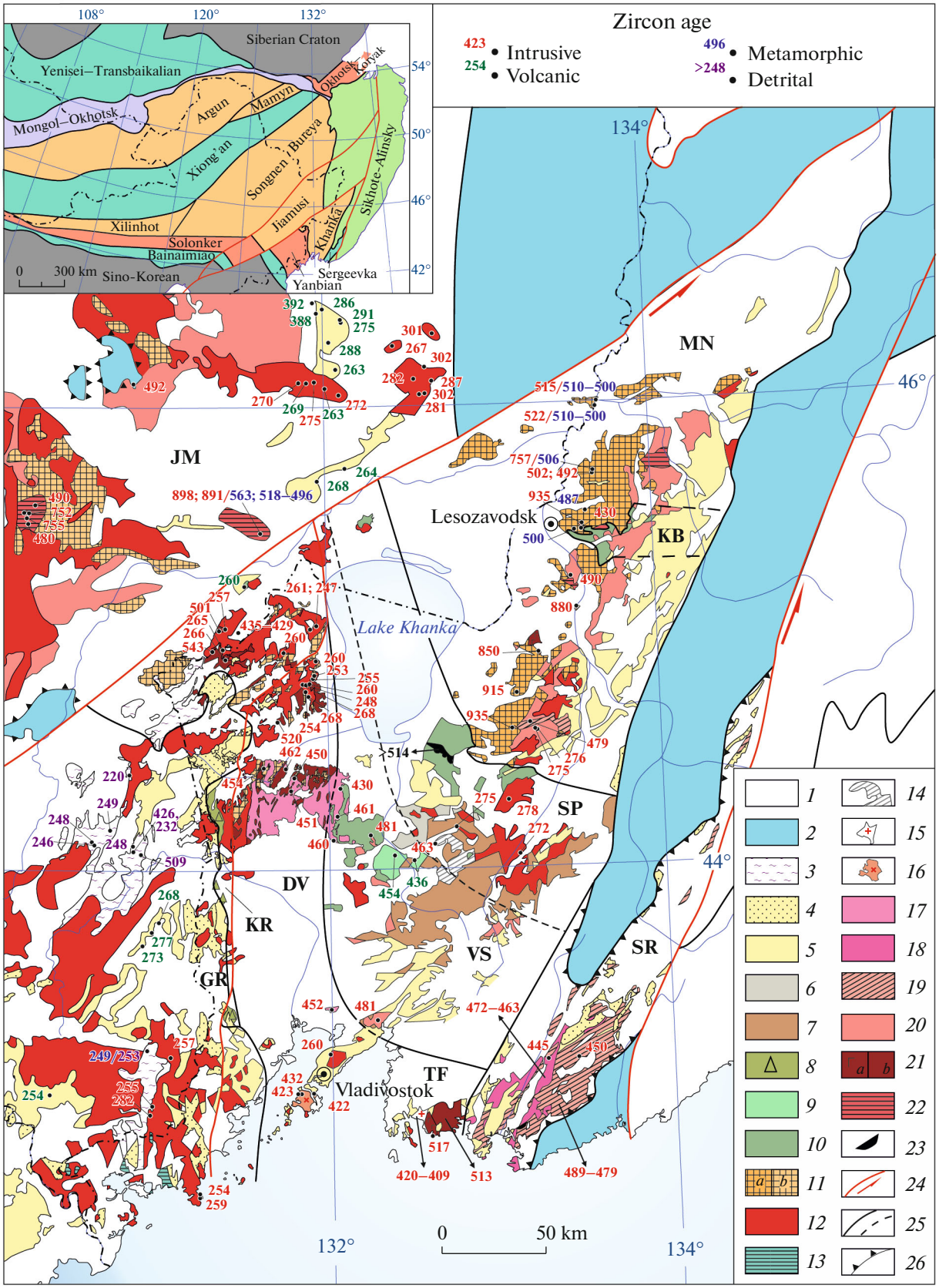
Zircon age
423 • Intrusive
254 • Volcanic
496 • Metamorphic
>248 • Detrital
108°
120°
132°
134°
54°
50°
46°
44°
42°
Siberian Craton
Yenisei–Transbaikalian
Mongol–Okhotsk
Argun
Mamyn
Okhotsk
Koryak
Xiong'an
Songnen
Bureya
Jiamusi
Khanka
Sikhote-Alinsky
Xilinhot
Solonker
Bainaimiao
Sino-Korean
Yanbian
Sergeevka
0 300 km
JM
MN
KB
SP
SR
DV
KR
GR
VS
TF
Lesozavodsk
Lake Khanka
Vladivostok
0 50 km
1
2
3
4
5
6
7
8
9
10
11
12
13
14
15
16
17
18
19
20
21
22
23
24
25
26

Botomian stages according to the Russian scale) [2–4, 27].[2] The Spassk zone differs in the presence of turbidites and terrigenous–mixtite sequences with trilobites of stages 4–5 (Toyonian and Amganian) in a matrix [27]. These rocks contain blocks of the older (according to Archeocyates) Fortunian (Tommotian) limestones and sheets of limestones of stages 2–3 (Atdabanian–Botomian) [2, 4, 27], olistoplacks, and olistoliths of cherts with Cambrian microfossils, and blocks of amygdaloidal basalts, gabbroids, and gabbrodolerites [10].

The oldest magmatic rocks are metavolcanic rocks and metaintrusions, which were metamorphosed to the same grade as host rocks [3]. The central part of the massif comprises ophiolitic dunites, harzburgites, pyroxenites, and olivine gabbronorites, which form several small lenticular, rarely irregularly shaped, bodies 0.5–7 km^2 in area [36, 48] in association with basalts and limestones of stage 3 (Botomian) [27]. Later Paleozoic deposits are mainly volcanogenic–sedimentary in composition and include supposedly Ordovician continental rhyolites and dacites dated at 454 and 436 Ma [29], Lower Silurian island-arc basalts and andesites [20, 21], Devonian continental, more rarely, shallow-water basic to felsic volcanic rocks, Lower Carboniferous continental rhyolites, as well as Permian basic–felsic volcanic rocks among shelf and shallow marine sedimentary rocks [3]. Early intrusions are Early Cambrian gabbros and granites with ages of 517 and 513 Ma, respectively, [17] and Late Cambrian–Early Ordovician granitods dated within 502–481 Ma [15, 16, 75, 94]. In southern Primorye, the widespread Sergeevka gabbro–diorite–gneiss complex [31] with age within 489–479 Ma [17] is intruded by 472–463-Ma granites [85] and 445-Ma trondhjemites [94]. Granitoids with an age of 460–450 Ma are distinguished in the western Khanka massif [14, 16, 45, 94]. There are also Silurian (432–422 Ma) [85, 94] and Devonian (420–409) [17] granitoid massifs. Late Permian–initial Triassic granitoids with ages from 275 to 250 Ma show ubiquitous distribution [14, 16, 29, 45, 94].

METHODS AND STUDIED OBJECTS

New analytical studies were carried out at the Center for Isotope Studies (CIS) of VSEGEI using certified technique. U–Pb SIMS zircon dating was conducted on a SHRIMP-IIe secondary ion microprobe [77]. Sm–Nd isotope analysis was carried out on a 9-channel TIMS TRITON mass spectrometer in static mode.

Locality and Description of Samples

Isotope-geochronological methods were used to study metagranitoids and metamorphic rocks in the northeast and metagranitoids in the west of the Khanka massif (Figs. 2, 3), as well as ophiolites in its central part.

[2] Hereinafter, according to the international and Russian scales.

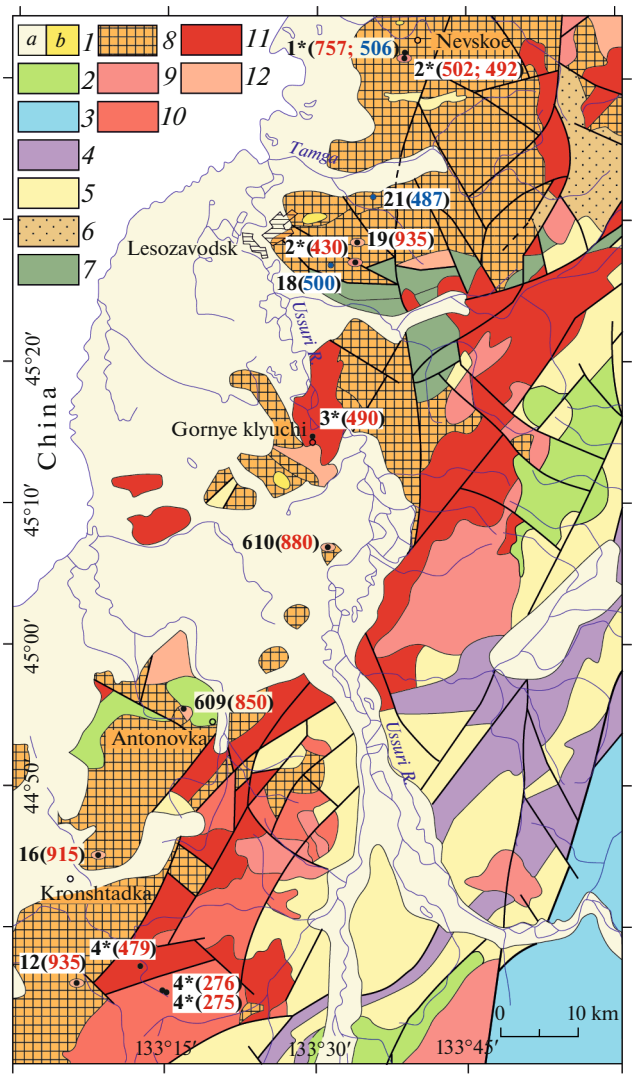

Fig. 2. The geological scheme of the northern part of the Khanka massif (modified after [3]). (*1*) Cenozoic sedimentary (a) and volcanic (b) deposits; (*2*) Cretaceous volcanogenic–sedimentary deposits; (*3*) Jurassic accretionary complex; (*4*) Upper Triassic sedimentary deposits; (*5*) Permian volcanogenic–sedimentary deposits; (*6*) Devonian sedimentary deposits (Tamga Formation); (*7*) Cambrian accretionary complex (unmetamorphosed) (Evgen'evskaya and Orlovka groups and Kabarga Formation); (*8*) Neoproterozoic metamorphic complex (Iman and Ussuri groups); (*9*) Cretaceous granites; (*10*) Permian granites (Bel'tsovsk Complex); (*11*) Late Cambrian–Early Ordovician granites (Shmakov complex); (*12*) Neoproterozoic granites. Circled numbers are sample numbers and age, in Ma, red color shows the age of magmatism, blue color shows the age of metamorphism. Numerals with asterisks are after: 1* [44]; 2* [94]; 3* [15]; 4* [29].

The metamorphosed intrusions in the Ussuri Group were united into the Ussuri gabbro–gneiss granite (predominant) complex. They form discordant or stratal bodies among host rocks and were metamorphosed together with them [3]. The granitoids show gneissosity with subparallel orientation of biotite and lenticular shape of quartz grains, without characteris-

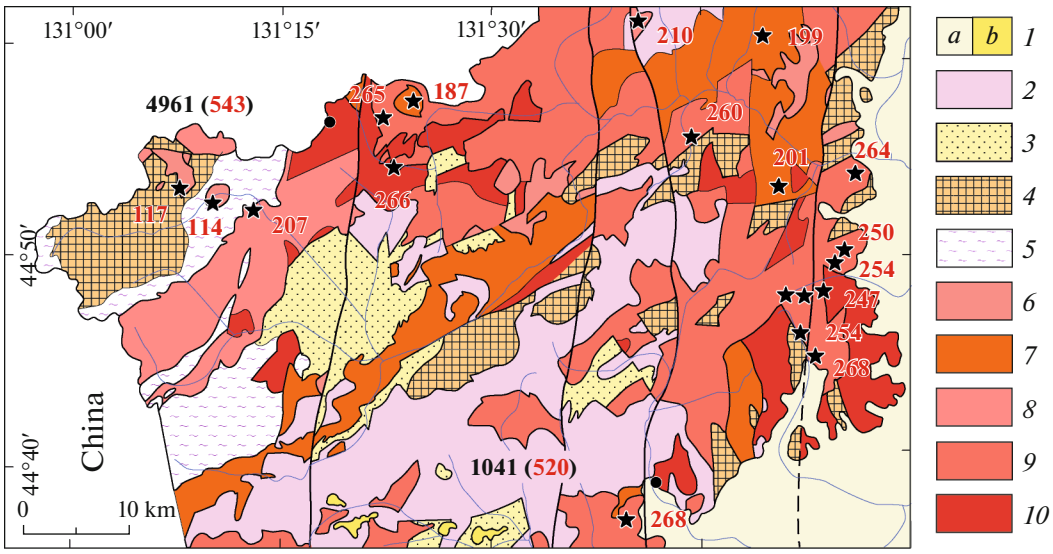

Fig. 3. The geological scheme of the northwestern part of the Khanka massif. (*1*) Neogene sedimentary (a) and flood basalt (b) deposits; (*2*) Upper Triassic dacites and rhyolites (Tal'ma sequence); (*3*) Permian sedimentary deposits (Reshetnikovskaya Formation); (*4*) Neoproterozoic–Early Cambrian protolith of the Late Cambrian schists, amphibolites, gneisses, quartzites, and marbles (Kraevskaya and Il'inka sequences); (*5*) Early–Middle Triassic micaceous schists and blastomylonites (tectonites); (*6*) Middle Cretaceous granites; (*7*) Early Jurassic granites; (*8*) Late Jurassic granites; (*9*) Late Permian granitoids; (*10*) Cambrian metagranitoids, more rarely gabbro (Dvoryan complex). Numerals are samples numbers and age of the intrusions, in Ma. Numerals with asterisks are the age of magmatism after [15].

tic metamorphic banding caused by differentiation into leucosome and melanosome, unlike gneisses of the Ussuri Group.

Sample 12 is a fine-grained gneiss granite collected from mine working (44°35′52.25″ N, 133°6′21.316″ E). The rock is made up of quartz, sodic oligoclase, K-feldspar, biotite, and garnet. In terms of major oxides (SiO_2, 69.5%), it is ascribed to high-Al (Al_2O_3, 16.3%), low-Ti (TiO_2, 0.21%) rocks of the mild-alkaline series of K alkalinity (K_2O/Na_2O = 1.9) and is classed as monzonite.

Sample 16 is a two-pyroxene granulite from the Tat'yanovka Formation (44°45′9.822″ N, 133°8′19.95″ E). This is a banded, fine-grained rock. Leucocratic minerals: andesine–secondary K-feldspar, and quartz. Melanocratic minerals (25–30 vol %) are diopside and orthopyroxene. The rock is high-Al (Al' = 2.13) and corresponds to the mild-alkaline potassic granite with 63.8 SiO_2, 0.66 TiO_2, 1.78 Na_2O, and 5.78 wt % K_2O.

Sample 609 is a biotite gneiss granite (44°55′27.616″ N 133°16′44.612″ E). It is composed of microcline, plagioclase, and quartz (up to 90%) and biotite. The granites are high-silica (SiO_2, 74.1%), moderately alkaline, with shift to the potassic region (alkali contents: K_2O, 5.46%; Na_2O, 2.6%). They have the moderate Al content (Al_2O_3, 13.6%), low contents of Fe, Mg, and Ti, and high contents of Li, Mo, and Sn.

Sample 19 is a gneiss granite (45°28′22.53″ N 133°34′1.548″ E). Leucocratic minerals are microclinized orthoclase–oligoclase and quartz aggregates, while melanocratic minerals are fine garnet grains and biotite flakes. Based on petrochemical features, the studied gneiss granites are classed as calc-alkaline K–Na, high-Al (Al' = 4.71) rocks, with SiO_2, 72.5 and $Na/K > 1$ (Na_2O, 3.43; K_2O, 3.15 wt %).

Sample 610 is gneiss granite collected from sequence of the Nakhimovka Formation (45°6′46.622″ N, 133°31′8.181″ E). It is made up mainly (up to 90%) of microcline, plagioclase, and quartz, with less common biotite. It differs in its high silica content (SiO_2, 77.3%), moderate Al_2O_3 (11.9%), low TiO_2 (<0.1%), low Fe mole fraction, and belongs to the low- to moderate alkali series of potassic alkalinity (K_2O/Na_2O = 2.7).

Metamorphic Rocks of the Iman and Ussuri Group

Sample 21 is a sillimanite–garnet–biotite–plagioclase schist from the Matveevka Formation (45°31′45.059″ N, 133°35′40.608″ E).

Sample 18 is a garnet–biotite–plagioclase gneiss of the Turgenevka Formation (45°26′52.692″ N, 133°31′16.782″ E).

Metagranitoids of the Dvoryan Complex

Sample 4961 is a metaplagiogranite (44°56′53.96″ N, 131°18′25.61″ E). It consists of quartz, oligoclase, with less common amphibole and biotite, and belongs to

the sodic series (SiO_2, 68.9; Al_2O_3, 17.2; K_2O, 2.56; and Na_2O, 5.56 wt %).

Sample 1041 is a gneiss granite (44°38′27.86″ N, 131°41′43.43″ E). The mineral assemblage includes quartz, oligoclase, K-feldspar (frequently perthites and antiperthites), with subordinate amphibole and biotite. The rock belongs to the K–Na series. SiO_2, 74.35; TiO_2, 0.19; Al_2O_3 13.63; Fe_2O_3, 1.00; FeO, 0.87; MgO, 0.19; CaO, 1.11; Na_2O, 3.50; and K_2O, 4.12 wt %.

Ophiolites

Sample 14 is an olivine metagabbronorite from the Dmitrievsky gabbroperidotite complex (44°27′746″ N, 132°41′418″ E). The rock is highly metamorphosed under nearly greenschist facies conditions and contains relicts of ortho- and clinopyroxene. SiO_2, 49.70; TiO_2, 0.29%; Al_2O_3, 14.80; Fe_2O_3, 2.48; FeO, 6.07; CaO, 10.70; Na_2O, 2.85; K_2O, 0.098 wt %. The rock is extremely depleted in rare-earth elements: ΣREE = 5.79 ppm. The REE content and distribution pattern, the degree of their fractionation (LREE/HREE = 0.9), as well as a weakly expressed positive Eu anomaly, are typical of mantle derivatives.

Sample 14/2 is almost completely metamorphosed peridotite (44°27′755″ N, 132°41′426″ E).

RESULTS OF GEOCHRONOLOGICAL STUDIES

Data on U–Pb isotopic ratios and age of the studied zircons are given in the Supplement to the on-line version of this paper.

Metamorphosed Intrusions in the Ussuri Group

Sample 12 is gneiss granite. This sample yielded transparent, mainly euhedral, long-prismatic zircons, with bipyramidal facets (Fig. 4). The length is 140–315 μm. The cathodoluminescence (CL) images of most grains show oscillatory zoning typical of magmatic zircons. Cores and growth zones are indiscernible. Some zircons have very thin light shells. Measurements were performed for 17 separate zircon grains. They have U = 162–837 ppm, Th/U = 0.28–0.63. The weighted average (14 analyses) concordant age is 935 ± 3 Ma. Oscillatory zoning and moderate Th/U ratio indicate a magmatic origin of the zircons [63]. The presence of thin shells around magmatic zircons is caused by metamorphic processes, which did not disturbed initial U–Pb system.

Sample 16 is a two-pyroxene granulite. Zircons in this sample are mainly subhedral. The grain size is 100–410 μm. Nine zircons were analyzed. Two of them contain 206 and 316 ppm U with Th/U ratios, respectively, of 0.22 and 0.32, which correspond to magmatic zircons with U–Pb concordant weighted average age of 916 ± 32 Ma and shell dated at 497 Ma. Other zircons (seven grains) with high U contents from 1708 to 3908 ppm (metamict zircon) and low Th/U ratios (0.02–0.06) have a distinct metamorphic genesis. The concordant U–Pb age of these zircons based on six measurements is 491 ± 7 Ma (Fig. 4). This age is interpreted as the age of complete recrystallization of primary magmatic zircons.

Sample 609 is a gneiss granite. Zircons are subeuhedral, short-prismatic. Their length is from 80 to 120 μm. In CL, the zircons show zoned structure, with core and metamorphic shells. Fifteen measurements were carried out. The concordant U–Pb age of 849 ± 20 Ma (Fig. 5) was obtained for cores of magmatic zircons (three grains) with traces of oscillatory zoning. Their magmatic genesis was confirmed by the presence of melt inclusions (Tolmacheva E.V., unpublished data). Zircon shells contain fluid inclusions. They define concordant age (based on six analyses) of 481 ± 4 Ma. The elevated contents of U from 1072 to 3283 ppm and Th from 609.4.2 to 3126 ppm in these zircons could be related to the uranium influx with fluid during metamorphic transformation. Thus, the Th/U ratios remain moderate from 0.1 to 0.39.

Sample 610 is a gneiss granite. Zircons in the sample are strongly modified. In CL, the crystals are mainly zoned and consist of cores and metamorphic shells with crystallized fluid inclusions. The cores contain melt, completely devitrified inclusions, which indicate their crystallization from magma. Fifteen analyses were performed. The zircons are characterized by the high U > 1000 ppm and a Th/U ratio from 0.02 to 0.51.

All age values are discordant. The upper-intercept age is 881 ± 4 Ma, which can be interpreted as the time of magmatic crystallization of zircon, subsimultaneously with sample 609 (Fig. 5).

Sample 19 is a gneiss granite. Zircons in the sample are long- and short-prismatic. The grains are 130–295 μm long. CL shows a weak oscillatory zoning. Nine zircons were analyzed. In grain 9, we dated the core at 934 ± 17 Ma and the shell at 723 ± 13 Ma (Fig. 5). The concordant U–Pb age of 935 ± 11 Ma was obtained for fine zircons (Fig. 5), four of which have U contents from 595 to 993 ppm, and one grain contains U = 3283 ppm, Th/U = 0.1–0.45, which is typical of magmatic zircons. In other four zircons with high U contents from 2232 to 6277 ppm and low Th/U = 0.08–0.24, the U–Pb isotope system of zircon was disturbed by metamorphic transformations. The upper-intercept age of 942 ± 10 Ma corresponds to the time of magmatic event.

Metamorphic Rocks of the Iman ad Ussuri Groups

Sample 21 is a sillimanite–garnet–biotite–plagioclase schist. Zircons from this sample are round, more rarely, elongate, 50–140 μm long. In CL, the zircons show a heterogeneous structure, with light

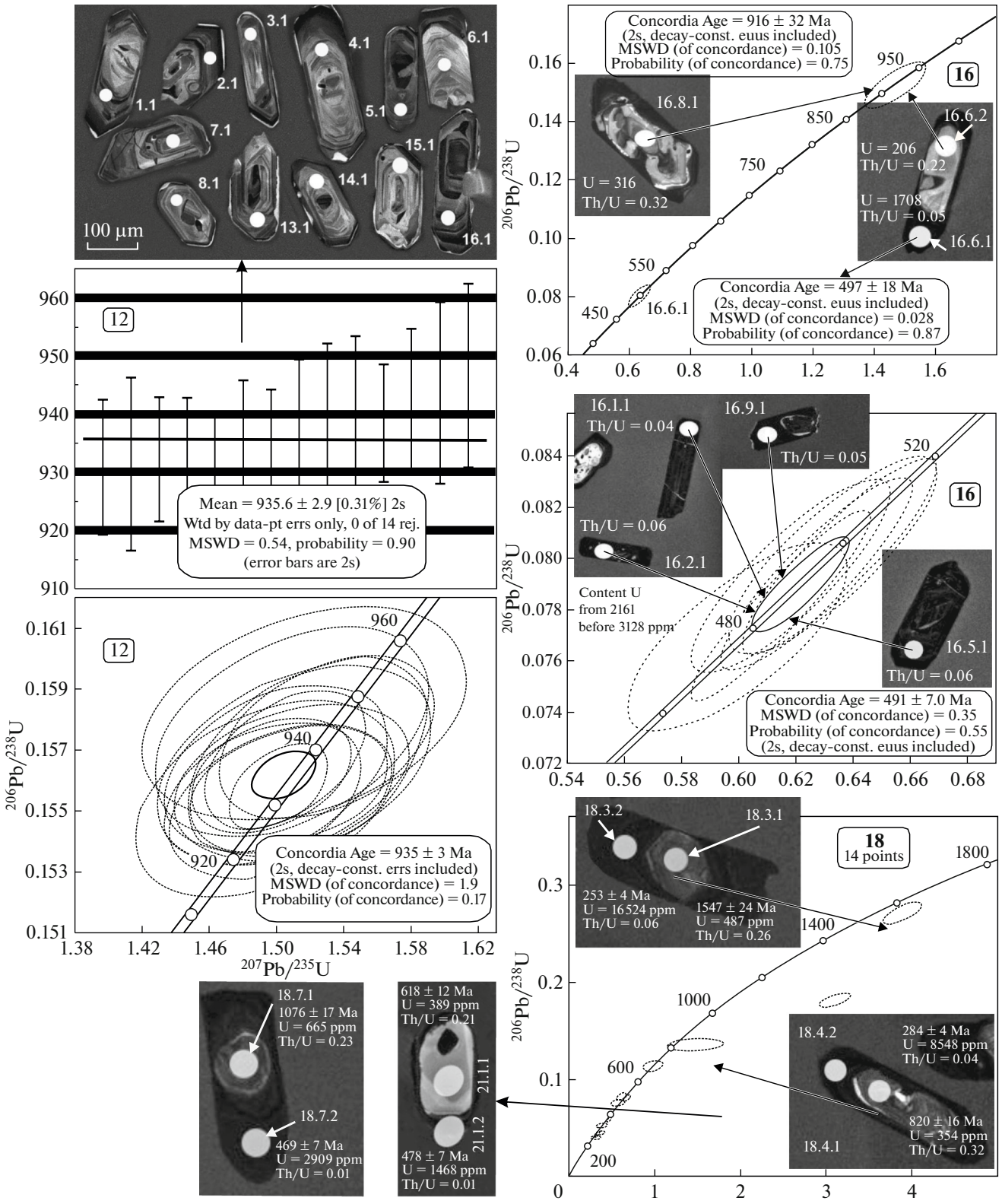

Fig. 4. CL microimages of typical zircon crystals, age histrogram, and U–Pb concordia diagram (sample 12), CL images of zircons and concordia diagrams for zircons from two-pyroxene granulite (sample 16), gneiss (sample 18), and metamonzonite (sample 21).

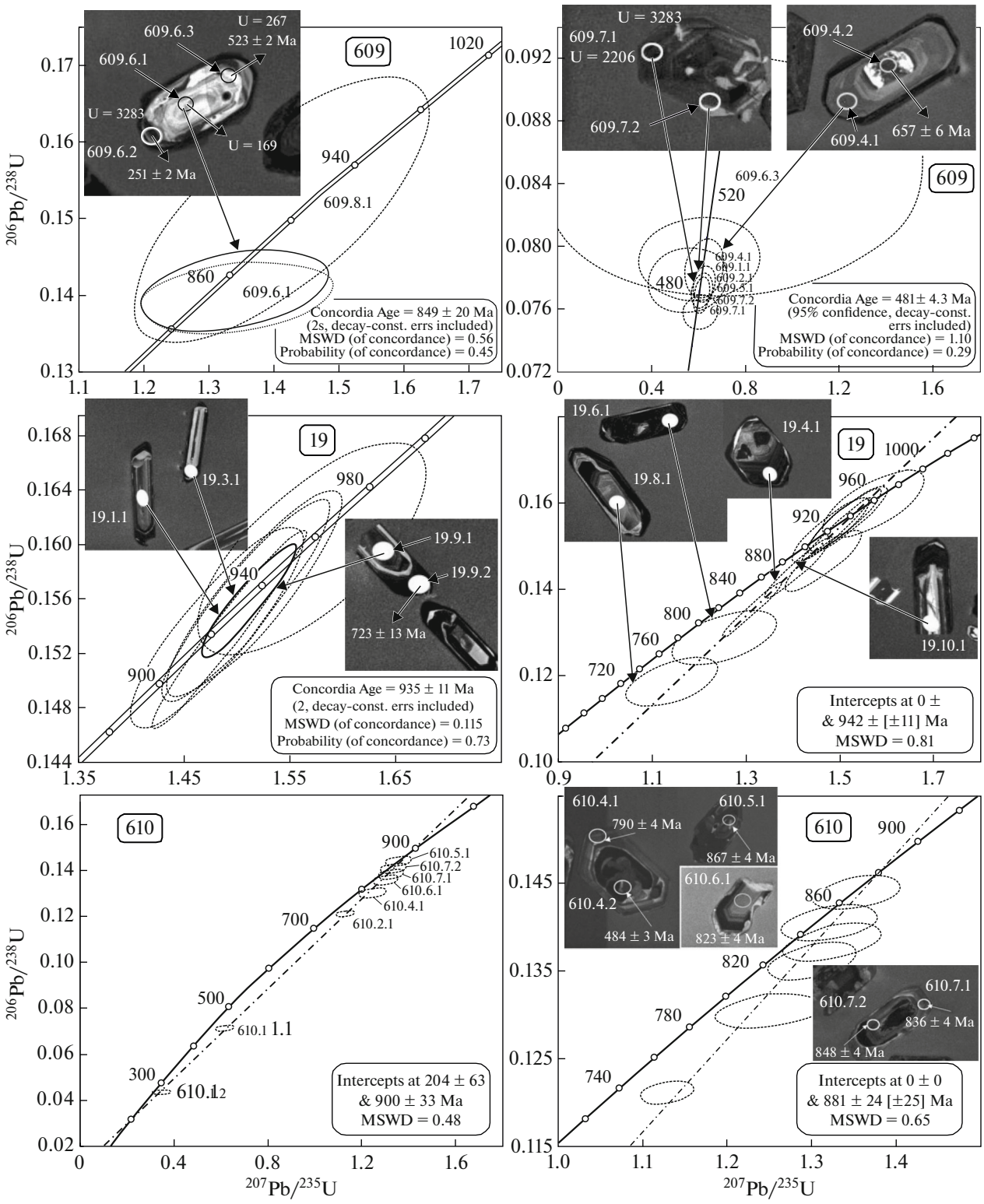

Fig. 5. CL images of zircon showing analysis spots in cores and shells and concordia diagrams for zircons from gneiss granites (samples 19, 609, 610).

The upper intercept of discordia, like concordant cluster, indicates the Neoproterozoic age of magmatism of gneiss granite sample 19.

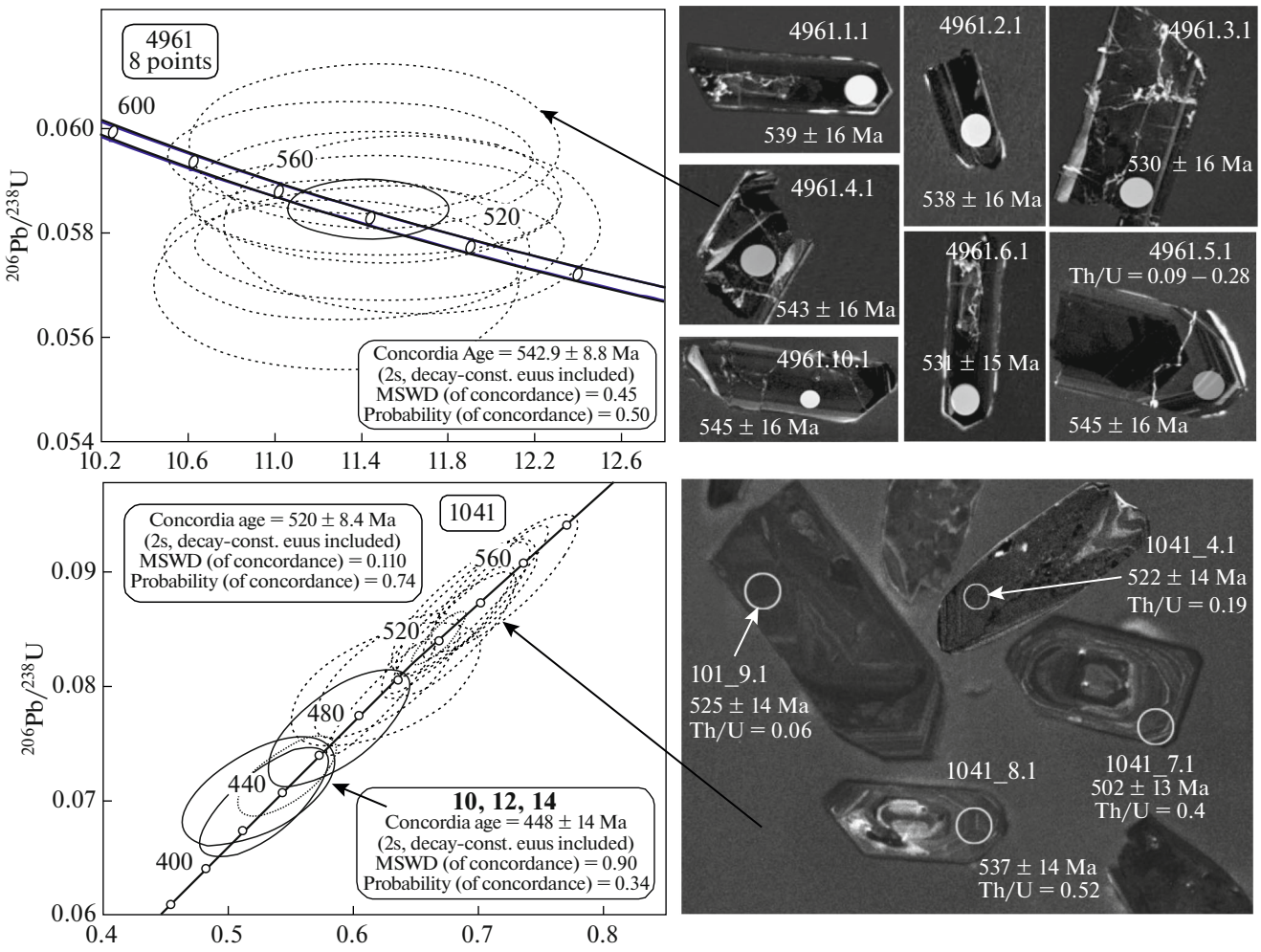

Fig. 6. Cathodoluminescence images of zircons and U–Pb concordia diagrams.

cores and dark shells in some grains. We analyzed eight zircons. Five zircons have high U = 1301–1868 ppm and low Th/U = 0.01–0.03. These zircons, likely of metamorphic genesis, define a concordant U–Pb age of 487 ± 6 Ma. Cores analyzed in two grains yielded ages of 677 ± 10 and 618 ± 12 Ma. Other three grains with moderate U contents (U = 783-991 ppm) and low Th concentrations Th (Th/U = 0.01–0.03) yield $^{206}Pb/^{238}U$ ages from 579 ± 8 to 514 ± 8 Ma, which likely reflects the intermediate stages of the transformation of the older zircons.

Sample 18 is a garnet–biotite–plagioclase gneiss of the Turgenevka Formation. In CL image, zircons from this sample are dark colored; some grains show light cores and traces of thin oscillatory zoning. We studied ten grains. In three zircons, we analyzed cores that have low U contents (U = 487–666 ppm) and moderate Th/U ratios (Th/U = 0.23–0.32) and shells with high U content, which is typical of all other zircons (U = 991–16524 ppm). The cores show discordant $^{206}Pb/^{238}U$ ages of 1547 ± 24, 1076 ± 17, and 820 ± 15 Ma. All features of the high-U zircons (Th/U = 0.01–0.12) indicate their polymetamorphic (metasomatic) genesis, with a wide scatter of dates from 250 to 500 Ma (Fig. 4).

Metagranitoids of the Dvoryan Complex

Sample 4961 is a gneiss granite. Zircons are fissured euhedral prismatic crystals with inclusions. The length is 100–300 μm. In CL (Fig. 6), the majority of zircons have oscillatory (magmatic) zoning. The weighted average concordant U–Pb age on eight zircons is 543 ± 9 Ma. These magmatic zircons are characterized by a high U = 1036–3108 ppm and low Th/U = 0.09–0.26.

Sample 1041 is a gneiss granite. Zircons from this sample are prismatic subeuhedral crystals from 130 to 360 μm in size. In CL image, zircons are dark colored, with traces of oscillatory zoning, while cores and shells of growth zones are weakly expressed (Fig. 6). Fifteen zircons define a concordant U–Pb crystallization age of 520 ± 8 Ma (9 grains) and two metamorphic stages

of their secondary recrystallization at 448±14 (three grains) and 244–296 Ma. Magmatic zircons have high U contents (U = 939–5312 ppm) and low Th/U ratios of 0.004–0.19, except for two zircons (7.1 and 8.1) of clearly expressed magmatic genesis with Th/U = 0.4–0.52. The U content in the metamorphic zircons varies from 375 to 1120 ppm (Th/U = 0.1–0.5).

Ophiolites

As mentioned above, ophiolites are olivine gabbronorites and peridotites. The absence of zircon in these rocks makes it impossible to apply U–Pb dating. Significant metamorphic transformations place constraints on Sm–Nd internal isochron dating. In our case, amphibole and whole-rock gabbronorite and peridotite were used for approximate Sm–Nd dating (Fig. 7, Table 1). A slope of three-point isochron corresponds to an age of 598 ± 84 Ma, which allowed us to constrain the upper age limit of the ophiolites at 514 Ma (Fig. 7).

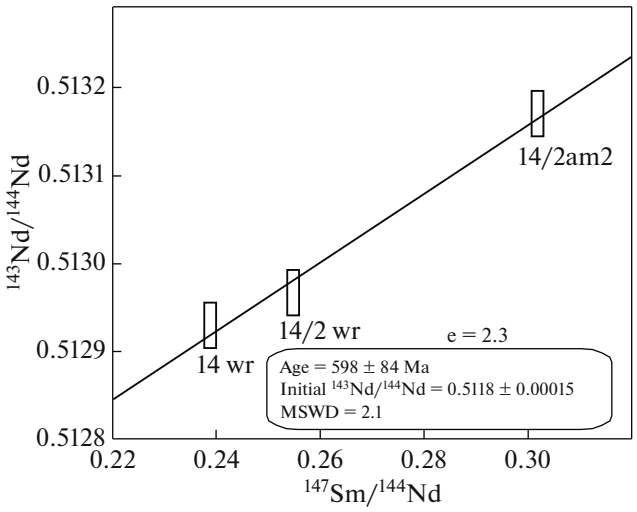

Fig. 7. The Sm–Nd amphibole and whole-rock isochron for gabbros and peridotites of the Dmitrievsky complex.

DISCUSSION OF THE RESULTS AND GEOLOGICAL CORRELATION

New Cambrian dates on metamorphic and magmatic zircons in the western part of the Khanka massif give us grounds to revise the scheme of its terrane structure [5, 43] and to distinguish a new Dvoryan terrane here made up of gneisses, crystalline schists, and amphibolites with lenses of quartzites and marbles (Kraevsky and Il'inka sequences). The Il'inka sequence is intruded by metadiorites and metagranodiorites, with subordinate orthoamphibolites (metagabbro) and gabbroamphibolites (Dvoryan complex), which are ascribed to the suprasubduction moderate-Al plutonic rocks of normal K–Na calc-alkaline series with low Nb content (5.33 ppm) [19] (Fig. 1). It is also necessary to distinguish the Kordonka terrane (Fig. 1), which is composed of volcanogenic-sedimentary complex. Finds of graptolites, brachyopodes, and trilobites indicate its Early Silurian (Late Llandoverian–Venlockian) age [20, 21]. Rock associations of the Kordonka terrane are typical of oceanic island arc with an accretionary wedge [21]. In addition, new data allowed us to divide the Sergeevka terrane into two terranes: the western Tafuin and eastern Sergeevka terranes. It should be noted that such subdivision was inferred previously based on finds of unique Permian Tethyan fauna, which is developed only in the Sergeevka (or Okrainsky) terrane [12 and references therein]. The Sergeevka terrane and its fragments to the north (including the Khorsky block) in the present-day structure represent a large tectonic nappe deformed together with underlying rocks of the Jurassic accretionary wedge [5, 43]. The Sergeevka terrane is considered as a part of a suprasubduction plate, which was separated and displaced along strike-slips [5].

The western boundary of the Khanka massif needs to be specified. The Neoproterozoic Kuban metamorphic complex (sequence) was distinguished in the Grodekovo (or Laoeling–Grodekovo) terrane, on the southwestern end of Primorye [18]. However, on the continuation of this complex in China (Wudagow Group), the age of metamorphic zircons was determined within 249–266 Ma, while the age of the youngest detrital zircons is 253 Ma, which indicates the Permian age of protolith [52]. Thus, the Kuban complex was metamorphosed in the Early Triassic. The northerly Huangsong metamorphic group was considered as the Precambrian basement of the Khanka massif. Recent studies of detrital zircons from the Huangsong Group showed that it represents a combination of tectonic nappes of different age, with age of the youngest populations of 220 Ma. Amphibolites yielded magmatic zircon with an age of 282 Ma. Given that the age of postmetamorphic intrusions is

Table 1. The results of Sm–Nd isotope analysis.

No.	Sample	Rock, mineral	Sm (ppm)	Nd (ppm)	$^{147}Sm/^{144}Nd$	$^{143}Nd/^{144}Nd$
1	14wr	Olivine gabbronorite, whole-rock	0.395	0.999	0.2388	0.512930 ± 6
3	14/2wr	Peridotite, whole-rock	0.147	0.348	0.2548	0.512967 ± 19
5	14/2am2	Amphibole 2	0.199	0.399	0.3019	0.513170 ± 26

~205 Ma, the age of last metamorphism of the Huangsong Group is 220–205 Ma (Late Triassic) [100].

It was shown that Middle Permian basalts from the lower part of the Barabash Formation in the area of the Barabash settlement have an oceanic origin and likely belong to the active-margin accretionary complex [6]. Early–Middle Permian (282–268 Ma) oceanic basalts and rhyolite complex (273–268 Ma) found to the north are considered to be originated through subduction of a spreading center beneath the accretionary wedge along the Khanka massif [88]. Hence, it is obvious that the Grodekovo terrane with its new boundary (Fig. 1) can be interpreted as the eastern part of the accretionary wedge in the Yanbian Fold Belt of Permian island-arc and accretionary complexes [51, 70, and references therein].

New geochronological data indicate a heterogeneity of the Khanka massif basement. Old block represented by the Matveevka–Nakhimovka terrane formed at the beginning of the Neoproterozoic can be distinguished in its northeastern part (Fig. 8). Stages of suprasubduction granitoid magmatism with ages of 935 ± 3, 935 ± 11, and 916 ± 32 Ma and within-plate or transform-margin magmatism with an age of 850–880 Ma were distinguished in this area. The granitoids clearly demonstrate the stages of zircon recrystallization within 480–490 Ma. Within-plate metabasalts with an age of 757 Ma and metamorphism of 506 Ma were previously described [44], while granite gneisses from the continuation of the Matveevka–Nakhimovka terrane in China yielded zircons with magmatic cores of 522 and 515 Ma and metamorphic shells with an age of 510– 500 Ma [102]. New age determinations of metamorphic events in the rocks of the Iman and Ussuri groups at 487 ± 6 and ~500 Ma are nearly similar to the formation ages of early postmetamorphic granitoids: 502, 492 [94], and 490 [15] Ma, which postdates the 506 Ma-old high-grade (up to granulite facies) regional metamorphism of the Matveevka–Nakhimovka terrane [44].

The stages of the Neoproterozoic magmatism of the Matveevka–Nakhimovka terrane coincide with the stages of basic and granitoid magmatism of 940–933 and 804–789 [42], 937–933 and 896–891 Ma [98] revealed in the eastern Bureya massif; 917–911 and 841 Ma [68], 929–927 and 895 Ma [69] in the Yichun block of the Jiamusi massif (authors ascribed this block to the Songnen massif); as well as the 898–891 Ma [96] and 757–751 Ma [97] in the Jiamusi massif. This is also consistent with conclusions of the cited authors about suprasubduction geochemical affinity of magmatism within 935–900 Ma and within-plate affinity of later magmatic rocks. It is pertinent to mention that the biotite and amphibole gneisses and amphibolites (metavolcanic rocks and metasediments), which host Early Neoproterozoic metagabbros and metagranitoids, in the Bureya massif, the Bureya River basin contain magmatic zircons with ages of ~950, ~940, and ~920 Ma [81]. Such a narrow age range of metavolcanic rocks and the coincidence with the age of metaintrusions suggest their initial formation in a suprasubduction volcanic island-arc setting. Thus, separate parts of the Khanka, Jiamusi, and Bureya massifs can be united into a single block with similar Neoproterozoic and Cambrian evolution (Fig. 8).

The Spassk and Voznesenka terranes of the accretionary and fore-arc complexes separated by conditional boundary are located to the southwest of the Matveevka–Nakhimovka terrane. The Spassk and Voznesenka terranes represent a closed oceanic basin (suture), which separates the Neoproterozoic Matveevka–Nakhimovka continental block and Dvoryan and Tafuin terranes of the Cambrian island arc. The upper age limit of ophiolites of the Dmitrievsky Complex is no more than 514 Ma, which is older than the upper age limit of the accretionary wedge, as follows from the find of Toyonian–Amganian trilobites [27] in its matrix. The closure of this oceanic basin likely occurred at the end of Precambrian, but the earlier orogenic granites have Early Ordovician ages of 481 ± 6 [16] and 481 ± 7 [75] Ma. The Early Cambrian deposits of the Voznesenka fore-arc and Spassk accretionary complexes (sutures) of terranes are correlated with coeval similar deposits from the Early Paleozoic fold belt. The belt was distinguished along the Zhangguangcai Range and in the southern part of the Lesser Xing'an Range, which is thought to separate the Precambrian Songnen and Jiamusi blocks, with allowance for the return of the Khanka massif in the prefault position [53, 84]. The Longfengshan ophiolite complex and suture are inferred in the middle–western part of the Zhangguangcai Range [66]. The Lesser Xing'an Range comprises the Lower Cambrian Chenming, Laodaomiaogou, and Wuxingzhen formations made up mainly of fine-grained terrigenous deposits and limestones. According to the characteristics of trilobites and brachyopods, the Wuxingzhen formation corresponds to stage 4 (Toyonian stage according to the Russian Scale) (~512–514 Ma). The Laodaomiaogou Formation comprises the Early Cambrian acritarchs, while the Chenming Formation contains microphytolites typical of the end of Ediacaran–beginning of Cambrian [76 and references therein]. These complexes are considered as deposits of the Late Neoproterozoic–Cambrian ocean and its margin [76]. The northern continuation of these complexes is the deposits of the Melgin zone at the Bureya massif. The oldest dated rocks (Melgin Formation) are made up of practically completely marbled limestones and dolomites with single intercalations of metasandstones and phyllite-like schists. The limestones comprise Ediacaran (Vendian) microphytolites [1, 30]. The younger deposits are coaly–clayey, sericite–cherty schists, siltstones, sandstones, with a thick limestone unit in the middle part of the sequence (Chergilen Formation) and sandstones and lenses (olistoplacks) of limestones (Allin Formation) [1, 30]. Archeocyates

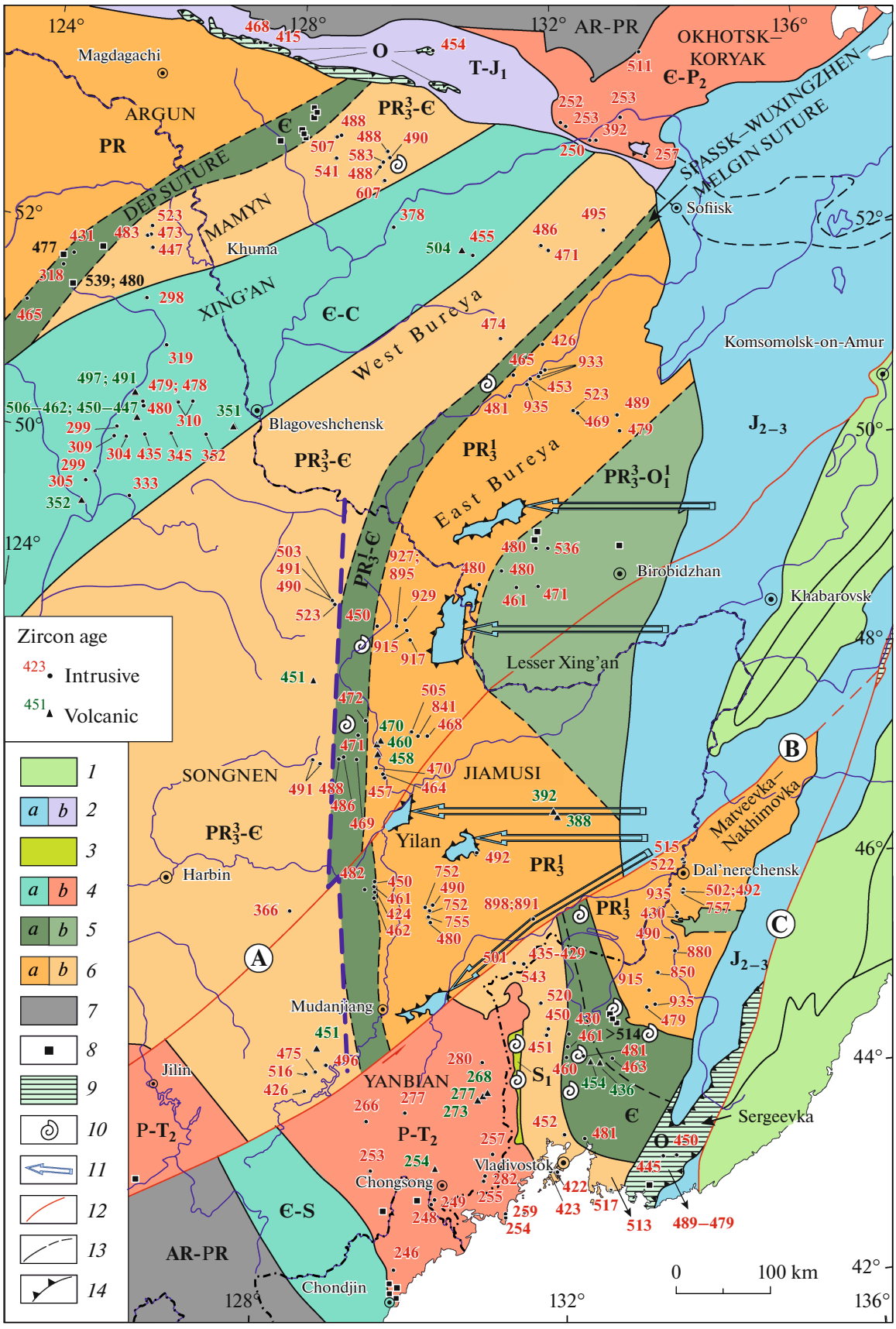
Zircon age
Intrusive
Volcanic
1
2
3
4
5
6
7
8
9
10
11
12
13
14
ARGUN
PR
DEP SUTURE
MAMYN
XING'AN
Є-C
West Bureya
East Bureya
PR$_3^3$-Є
PR$_3^1$
PR$_3^3$-O$_1^1$
J$_{2-3}$
T-J$_1$
Є-P$_2$
SPASSK–WUXINGZHEN–MELGIN SUTURE
OKHOTSK–KORYAK
AR-PR
Є-S
P-T$_2$
S$_1$
O
Є
SONGNEN
JIAMUSI
YANBIAN
Lesser Xing'an
Matveevka–Nakhimovka
A
B
C
Magdagachi
Khuma
Blagoveshchensk
Sofiisk
Komsomolsk-on-Amur
Birobidzhan
Khabarovsk
Harbin
Yilan
Dal'nerechensk
Mudanjiang
Jilin
Chongsong
Vladivostok
Sergeevka
Chondjin
124°
128°
132°
136°
52°
50°
48°
46°
44°
42°
0
100 km

of stage 2 (Middle Atdabanian and Late Atdabanian) were found in limestones of both formations [2]. In addition, the terrigenous sequence with blocks of quartzites, marbled limestones, and metabasalts distinguished in the Melgin zone [1] is comparable to the accretionary wedge. This is consistent with the conclusion that the Early Cambrian terrigenous deposits were accumulated in an active continental margin setting [25]. Archeocyates of stage 2 (Atdabanian) of the Melgin zone are identical to archeocyates of the Spassk terrane, while their species composition suggests that they were formed in a single oceanic basin in the vicinity of and on the Gondwana margin [4]. The data presented above allowed us to recognize the Spassk–Wuxingzhen–Melgin (SWM) suture (Fig. 8).

The Dvoryan terrane is located in the southwestern part of the Khanka massif. As shown above, the early metagranitoids of suprasubduction type have ages of 543 ± 9 and 520 ± 8 Ma, while high-grade metamorphism is dated at 503 ± 20 Ma. The values of εHf (*t*) in zircons are positive in the Ordovician granitoids in the Dvoryan terrane and negative in the Matveevka–Nakhimovka terrane, which marks a relatively younger age of continental crust of the Dvoryan terrane [94].

In the Chinese part of the Dvoryan terrane, the age of suprasubduction gabbro is determined as 501 Ma [95]. This area also comprises suprasubduction gabbro with an age of 435–429 Ma [99], which is comparable with the age of the Kordonka island-arc terrane. Thus, the Dvoryan terrane can be considered as a fragment of the Cambrian ensialic crust. It should be noted that amphibolite collected at a depth of 190 m from hole drilled in the Chinese portion of the Dvoryan terrane yielded Late Neoarchean magmatic zircons (~2.54 Ga), the age of which is considered as the protolith age, thus suggesting the presence of the Archean basement [60]. However, this is inconsistent with other data and requires additional studies.

A direct northern continuation of the Dvoryan terrane with a westward shift along the strike-slip line is the Tadong Group of the Songnen massif, where the protolith age of the amphibolite- and granulite-facies metamorphic rocks is determined within 750–516 Ma [87], while the ages of suprasubduction metatonalites and tonalites are 516 and 426 Ma [89]. Thus, the Dvoryan terrane can be considered as the southern continuation of the eastern part of the Songnen massif, which is consistent with conclusion made from comparison of ages of detrital zircons. [93, 100].

The distinguished SWM suture divides the Bureya massif into two parts: the Early Neoproterozoic East Bureya terrane to the southeast of the suture (Fig. 8), and the West Bureya terrane to the northwest. The latter is located on the continuation of the Dvoryan terrane and the northeastern part of the Songnen massif. In the West Bureya terrane, the youngest detrital zircons in the metaterrigenous deposits of the upper part of the sequence have an age of 483 Ma [39]. In gneisses, peaks in the relative-age probability diagram correspond to 487, 541, 690, 778, and 896 Ma. Zircons with an age older than 1 Ga are absent. The lower age limit of protolith accumulation is Late Cambrian, ~487 Ma, based on the young population [26]. To the south, the SWM suture should be considered as the boundary between the Songnen and Jiamusi massifs. In this interpretation, the boundary of the Jiamusi massif is shifted to the west and it joins the Early Proterozoic Yichun miniblock previously ascribed to the Songnen massif [66, 68, 69]. This is consistent with Hf model ages on zircons in the Phanerozoic granitoids, which suggests that the boundary of the older Jiamusi province is shifted for ~130 km west of the previously accepted boundary along the modern Mudanjiang fault between the Jiamusi and Songnen massifs: TDM2 Hf (1.6–1.1) and 1.1–0.4 Ga, respectively. This indicates a sharply different nature of the Precambrian basement beneath these two blocks [57]. Moreover, the Jiamusi massif experienced granulite-facies metamorphism at 540 Ma, which suggests that the Songnen and Jiamusi blocks separate continental blocks with different tectonic history up to ~540 Ma [61 and references therein]. This conclusion is consistent with our data on the 543-Ma age of suprasubduction granitoids in the Dvoryan terrane as the continuation of the Songnen massif. The most part of the Songnen massif is overprinted by the Mesozoic Songliao basin, and structure of its basement is hotly debatable. The traditional concepts on the ubiquitous distribution of the Precambrian basement in this area

Fig. 8. The tectonic scheme of the basement of continental part of East Asia and age of early magmatic rocks. Age of zircons after data from [14–17, 24, 25, 32, 34, 36–40, 42, 44, 45, 50–52, 55, 56, 63, 66, 67, 69, 70, 72, 73, 75, 79, 80, 83, 85, 88, 92, 94, 96–99, 102, and others]. (1) Early Cretaceous terranes of fragments of the accretionary wedges, turbidite basin, and island arc; (2) terranes of accretionary wedges of the Middle–Late Jurassic with fragments of Devonian–Early Jurassic oceanic plate (a), of the Triassic–Early Jurassic with fragments of Devonian–Permian oceanic plate (b); (3) Early Silurian island-arc terrane; (4) orogenic belts and terranes with accretionary (including ophiolites and paleooceanic basalts) and island-arc complexes, synkinematic granitoids, and metamorphic complexes of Paleozoic (a) and Permian–Triassic (b); (5) terranes of accretionary wedges and shelf complexes of the Ediacaran–Cambrian sutures (a) and Ediacaran–Early Ordovician continental margins (b); (6) continental massifs of the early (a) and late (b) Neoproterozoic; (7) cratons; (8) ophiolites; (9) Ordovician gabbro-granite remnants on the Mesozoic accretionary wedges; (10) valid Cambrian or Early Silurian fauna; (11) continuation of the Sikhote-Alin accretionary wedge in the tectonic windows of the Heilongjiang Complex as result of Early Cretaceous deformations after gentle Jurassic subduction; (12) Early Cretaceous sinistral strike-slips: (A) Yilan–Yichun; (B) Dunhua–Mishan, (C) Central Sikhote Alin; (13) tectonic boundaries; (14) contours of tectonic windows or allochthons. Dashed violet line is the boundary of Phanerozoic granitoid provinces with TDM2 Hf (1.6–1.1) to the east and 1.1–0.4 Ga to the west after [57].

have been revised. The wide distribution of newly formed Paleozoic continental crust is inferred. The exception is the Xilinhot block with ancient ages within 739–1399 Ma [66].

One can suggest that the collision of the Jiamusi continental block (including the Matveevka–Nakhimovka and East Bureya terranes) and Songnen island-arc block (including the Dvoryan and West Bureya terranes) occurred in the terminal Cambrian. This collision likely began from the juxtaposition of the northern parts of the massifs, as follows from the manifestation of syn- and post-collision mainly A-type granites with an age of 523–490 Ma in the Songnen massif [61]. In the north, in the West Bureya terrane, the oldest post-collision granites (A2-type) have an age ~495–486 Ma [73]. In the south, the age of collision and post-collision granitoids west of SWM suture decreases from the north southward from 505–496 to 496–482 ([89] and references therein), reaching 481 Ma on its termination [16, 75].

The Kabarga terrane made up of the alternation of terrigenous deposits with bodies of basalts, quartzites, and limestones is considered as a fragment of the accretionary wedge. The deposits of this terrane are correlated with the upper part of the Xing'an Group [3] composed of the Vendian–Cambrian deposits (Iginchin, Murandav formations and Kimkan sequence) [9] of the Lesser Xing'an terrane [5]. A thin (110 m) rhyolite horizon was distinguished in the lower, terrigenous–carbonate subformation of the Murandav Formation [9]. In addition, the terrigenous deposits of the Murandav Formation are cut by dike bodies (up to 4 m thick) of gneissic hornblende granites with an age of 535 Ma [41], while detrital zircons from the Murandav and underlying Iginchin Formation yield Late Riphean–Vendian ages [35]. The upper subformation of the Murandav Formation and Kimkan sequence, in addition to the ore-bearing jasper-like cherts, contains enclaves of jaspers, limestones, and quartzites (metacherts) [9, 30] of paleooceanic origin [46], which allows the correlation of the upper part of the Xing'an Group with accretionary wedge. This is consistent with the age difference between limestone enclaves and the terrigenous matrix typical of the accretionary wedge, which was established in the Kimkan Sequence. The limestones based on paleontological data has the Early Cambrian age [9], whereas its matrix yielded detrital zircons with Late Cambrian–Early Ordovician age (up to 481 Ma) [35]. In general, weakly metamorphosed rocks of the Lesser Xing'an terrane are comparable with complexes of different age of the transform (Ediacaran–Lower Cambrian shelf deposits with limited magmatism) and convergent margins (Cambrian–Early Ordovician accretionary wedge) of the Pacific type.

Unlike the main part of the Khanka massif, the terminal Permian fauna in the Sergeevka terrane is Tethyan, similar to that of the South China [11, 62]. The taxonomic composition of pre-Albian floral assemblages sharply differs: boreal at the Khanka massif and subtropical at the Sergeevka terrane. This suggests that the Sergeevka terrane, together with the Jurassic accretionary wedge, could ave experienced significant (by >15°) displacements from the south northward [58]. This conclusion is confirmed by studies of detrital zircons from Devonian and Permian sandstones near the town of Nakhodka, which are correlated to the zircon population in the eastern Japan and indicate the relation with South China [62].

The new age data on the oldest complexes of the Khanka massif and regional correlations are consistent with concepts that the BSJK superterrane was formed as a part of the Gondwana supercontinent near 500 Ma owing to orogenesis and accretion of fragments of the Rodinia supercontinent [8, 66, 95, 97, 102, and others].

CONCLUSIONS

The new and previously published geochronological data indicate that the basement of the Khanka massif has a heterogeneous structure. The Early Neoproterozoic Matveevka–Nakhimovka terrane with early suprasubduction magmatism with ages of 935 ± 3, 935 ± 11, ~915 Ma and within-plate or Pacific-type transform margin magmatism with ages of 850–880 and 757 Ma, as well as early regional metamorphism of 506 and 500 Ma are distinguished in its northeastern part. The southwestern part comprises Late Neoproterozoic–Early Cambrian Dvoryan and Tafuin terranes with suprasubduction magmatism dated at 543 ± 9 Ma, 520 ± 8, 517, and 513 Ma. These two parts are separated by suture (Voznesenka and Spassk terranes) formed by the Cambrian shelf deposits and accretionary wedge with ophiolites older than 514 Ma. The Kabarga terrane is a fragment of accretionary wedge of supposedly Cambrian age. The formation of most part of the Khanka massif occurred in the terminal Cambrian. At the end of the Silurian, the Early Silurian Kordonka island-arc terrane was accreted to it. The Ordovician Sergeevka island-arc terrane joined the Khanka massif owing to the Albian–Cenomanian strike-slip displacement.

Based on the ages of early magmatic and metamorphic stages, heterogeneous structures of the main part of the Khanka massif are traced to the north, where the Jiamusi massif (including its East Bureya terrane) represents the Early Neoproterozoic block, while the eastern part of the Songnen massif (including the West Bureya terrane) is the Late Neoproterozoic–Cambrian block. These blocks are separated by the Spassk–Wuxingzhen–Melgin (SWM) suture that formed during their collision.

The Bureya–Songnen–Jiamusi–Khanka superterrane was formed as a part of the Gondwana super-

continent at 500 Ma through orogenesis and accretion of fragments of the Rodinia supercontinent.

ACKNOWLEDGMENTS

We are grateful to N.N. Kruk and corresponding member of the RAS A.A. Sorokin for critical comments, which significantly improved the manuscript. O. I. Kenya is thanked for help with graphical works.

FUNDING

Results of geochronological study were obtained in the framework of the government-financed program of VSEGEI (no. AL-02–06/35) and the government-financed programs of the Federal Agency on Nature Management on December 26, 2019 (no. 049-00017-20-04) and on January 14, 2021 (no. 049-00016-21-00). Collection and processing of information were financially supported by the Russian Science Foundation (project no. 21-77-20022), while edition of the paper was supported by the Russian Foundation for Basic Research (project no. 19-05-00229).

CONFLICT OF INTEREST

The authors declare that they have no conflicts of interest.

SUPPLEMENTARY INFORMATION

The online version contains supplementary material available at https://doi.org/10.1134/S1819714022040042 and are accessible for authorized users.

Supplementary data to this paper are available at http:/itig.as.khb.ru/POG/2022/2022_N41_T4.html.

REFERENCES

1. V. N. Arapov, S. A. Amelin, A. F. Atrashenko, et al., *Report on the Results of Works on the Object "GDP-200 of Sheet M-52-XII (Melgin Area)*, (Dal'geofizika, Khabarovsk, 2016) [in Russian].
2. G. V. Belyaeva, *Cambrian of Eastern USSR* (Nauka, Moscow, 1988) [in Russian].
3. G. S. Belyanskii, V. I. Rybalko, A. A. Syas'ko, et al., *Geological Map of the Russian Federation. 1 : 1000000 (Third Generation). Sheet (L-(52), 53; (K-52, 53). Lake Khanka: Explanatory Note* (VSEGEI, St. Petersburg, 2011) [in Russian].
4. L. G. Bondarenko and I. V. Kemkin, "Spatiotemporal relations of Early Cambrian basins of Siberia and Far East: evidence from distribution of the Tumul," Vestn. KRAUNTs. Nauki O Zemle, No. 1, 42–53 (2009).
5. *Geodynamics, Magmatism, and Metallogeny of East Russia*, Ed. by A. I. Khanchuk (Dal'nauka, Vladivostok, 2006) [in Russian].
6. V. V. Golozubov, N. N. Kruk, V. I. Kiselev, S. N. Rudnev, S. A. Kasatkin, E. A. Kruk, "First evidence for the Middle Triassic volcanism in South Primorye," Russ. J. Pac. Geol. **11** (2), 110–122 (2017).
7. V. V. Golozubov and A. I. Khanchuk, "The Heilongjiang complex as a fragment of a Jurassic accretionary wedge in the tectonic windows of the overlying plate: a flat slab subduction model," Russ. J. Pac. Geol. **15** (4), 279–292 (2021).
8. A. N. Didenko, A. A. Mossakovskii, D. M. Pecherskii, S. V. Ruzhentsev, S. G. Samygin, and T. N. Kheraskova, "Geodynamics of Paleozoic oceans of Central Asia," Geol. Geofiz. **35** (7-8), 59–75 (1994).
9. S. N. Dobkin, *State Geological Map of the Russian Federation. 1 : 200000. Bureya Series. Sheet M-52-XXX. Explanatory Note* (VSEGEI, Moscow, 2016) [in Russian].
10. I. V. Kemkin and V. S. Rudenko, "The first find of Early Paleozoic siliceous microfossils in olistoliths of the Spassk accretion prism (Western Primor'e)," Dokl. Earth Sci. **357A** (9), 1269–1271 (1997).
11. G. V. Kotlyar, "Permian sections of southern Primorye: a link in correlation of stage units in the standard and general stratigraphic scales," Russ. J. Pac. Geol. **9** (4), 254–273 (2015).
12. A. B. Kotov, S. D. Velikoslavinskii, A. A. Sorokin, L. N. Kotova, A. P. Sorokin, A. M. Larin, V. P. Kovach, N. Yu. Zagornaya, and A. V. Kurguzova, "Age of the Amur Group of the Bureya–Jiamusi superterrane in the Central Asian Fold Belt: Sm–Nd isotope evidence," Dokl. Earth Sci. **429** (8), 1245–1248 (2009).
13. N. N. Kruk, V. P. Kovach, V. V. Golozubov, S. A. Kasatkin, L. B. Terent'eva, and S. N. Lavrik, "Nd isotope systematics in metamorphic rocks of the southern Russian Far East," Dokl. Earth Sci. **455** (1), 233–237 (2014).
14. N. N. Kruk, V. V. Golozubov, S. N. Rudnev, A. A. Vrzhosek, S. A. Kasatkin, M. L. Kuibida, and G. M. Vovna, "Granitoids of the Gamov intrusion (southern Primorye), its peculiarities and indicator and geodynamic role," Russ. Geol. Geophys. **56** (12), 1685–1700 (2015).
15. N. N. Kruk, V. V. Golozubov, T. B. Bayanova, and S. A. Kasatkin, "Composition, age, and tectonic position of granitoids of the Shmakovka Complex," Russ. J. Pac. Geol. **10** (2), 132–140 (2016).
16. N. N. Kruk, V. V. Golozubov, V. I. Kiselev, E. A. Kruk, S. N. Rudnev, P. A. Serov, S. A. Kasatkin, and E. Yu. Moskalenko, "Paleozoic granitoids of the southern part of the Voznesenka Terrane (Southern Primorye): age, composition, melt sources, and tectonic settings," Russ. J. Pac. Geol. **12** (3), 190–209 (2018).
17. N. N. Kruk, V. V. Golozubov, A. I. Khanchuk, I. A. Aleksandrov, A. A. Chashchin, and E. V. Sklyarov, *Intrusive Complexes of the Sergeevka Terrane—the Oldest Block of Southern Primorye* (Dal'nauka, Vladivostok, 2018) [in Russian].
18. T. K. Kutub-Zade, S. V. Kovalenko, A. M. Korotkii, et al., *State Geological Map of the Russian Federation. 1 : 200000. Khanka Series. Sheet K-52-XI, XVII: Explanatory Note* (MF VSEGEI, Moscow, 2013) [in Russian].
19. T. K. Kutub-Zade, A. T. Kandaurov, V. I. Rybalko, et al., *State Geological Map of the Russian Federation. 1 : 200000. 2nd Edition. Khanka Series. Sheet L-52-XXX (Il'inka):*

Explanatory Note (MF VSEGEI, Moscow, 2020) [in Russian].

20. T. K. Kutub-Zade, A. T. Kandaurov, V. I. Rybalko, et al., *State Geological Map of the Russian Federation. 1 : 200000. 2nd Edition. Sheet L-52-XXXVI (Pogranichnyi): Explanatory Note* (MF VSEGEI, Moscow, 2020) [in Russian].
21. A. I. Malinovsky and V. V. Golozubov, "Lower Silurian terrigenous rocks of the Laoeling–Grodekovo terrane, southern Primorye: composition and formation settings," Russ. J. Pac. Geol. **15** (1), 1–19 (2021).
22. M. A. Mishkin, *Petrological Precambrian Metamorphic Complexes of the Khanka Massif, Primorye* (Nauka, Moscow, 1969) [in Russian].
23. M. A. Mishkin, A. I. Khanchuk, D. Z. Zhuravlev, and S. N. Lavrik, "First data on the Sm–Nd systematics of metamorphic rocks in the Khankai Massif, Primor'e region," Dokl. Earth Sci. **375** (8), 1283–1285 (2000).
24. R. O. Ovchinnikov, A. A. Sorokin, and N. M. Kudryashov, "Age of the Early Precambrian (?) intrusive complexes of the northern Bureya continental massif, Central Asian Fold Belt," Russ. J. Pac. Geol. **12** (4), 289–302 (2018).
25. R. O. Ovchinnikov, A. A. Sorokin, V. P. Kovach, and A. B. Kotov, "Geochemical features, sources, and geodynamic settings of accumulation of the Cambrian sedimentary rocks of the Mel'gin Trough (Bureya Continental Massif)," Geochem. Int. **57** (5), 540–555 (2019).
26. R. O. Ovchinnikov, A. A. Sorokin, V. P. Kovach, and A. B. Kotov, "Late Paleozoic age and nature of protolith of metamorphic rocks of the Djagdagle Formation, Bureya terrane, Central Asian Fold Belt," Stratigraphy. Geol. Correlation **28** (3), 250–262 (2020).
27. O. G. Okuneva and L. N. Repina, *Cambrian Biostratigraphy and Fauna of Primorye* (Nauka, Novosibirsk, 1973) [in Russian].
28. L. M. Parfenov, N. A. Berzin, A. I. Khanchuk, G. Badarch, V. G. Belichenko, A. N. Bulgatov, S. I. Dril', G. L. Kirillova, M. I. Kuzmin, W. D. Nokleberg, A. V. Prokop'ev, O. Tomurtogoo, and H. Jan, "Model of formation of orogenic belts of the central and northeastern Asia," Tikhookean. Geol. **22** (6), 7–41 (2003).
29. O. V. Petrov, A. F. Morozov, T. V. Chepkasova, and S. S. Shevchenko, *Geochronological Atlas—Reference Book of Main Lithotectonic Compelxes of Russia* (VSEGEI, St. Petersburg, 2015) [in Russian].
30. N. N. Petruk, Yu. R. Volkova, M. N. Shilova, A. V. Myalik, et al., *State Geological Map of the Russian Federation. 1 : 1000000 (Third Generation). Sheet M52. Blagoveshchensk: Explanator Note* (VSEGEI, St. Petersburg, 2012) [in Russian].
31. S. M. Sinitsa and A. I. Khanchuk, "Primary Gneissic Facies in Gabbroids: Evidence from the Southern Primorye," Dokl. Akad. Nauk SSSR **317** (6), 1446–1449 (1991).
32. Yu. V. Smirnov, A. A. Sorokin, A. B. Kotov, E. B. Sal'nikova, S. Z. Yakovleva, and B. M. Gorokhovskii, "Early Paleozoic monzodiorite–granodiorite association in the northeastern flank of the south Mongolia–Khingan Orogenic Belt (Nora–Sukhotinsky Terrane): age and tectonic setting," Russ. J. Pac. Geol. **10** (2), 123–131 (2016).
33. Yu. V. Smirnov and A. A. Sorokin, "Geochemical and Sm–Nd isotope–geochemical patterns of metavolcanic rocks, diabase, and metagabbroids on the northeastern flank of the South Mongolian–Khingan Orogenic Belt," Dokl. Earth Sci. **474** (1), 574–578 (2017).
34. Yu. V. Smirnov, A. A. Sorokin, and N. M. Kudryashov, "First evidence for Late Devonian granitoid magmatism in the evolution of the noreastern flank of the South Mongolian–Xing'an Orogenic Belt," Tikhookean. Geol., 2022. (in press).
35. Yu. N. Smirnova, A. A. Sorokin, A. B. Kotov, and V. P. Kovach, "Tectonic conditions of sedimentation and source areas of Upper Proterozoic and Lower Paleozoic terrigenous deposits of the Lesser Khingan terrane of the Central Asian Fold Belt," Stratigraphy. Geol. Correlation **24** (3), 219–241 (2016).
36. A. A. Sorokin, A. B. Kotov, E. B. Sal'nikova, N. M. Kudryashov, and V. P. Kovach, "Early Paleozoic gabbro-granitoid associations in eastern segment of the Mongolian–Okhotsk Foldbelt (Amur River Basin): age and tectonic position," Stratigraphy. Geol. Correlation **15** (3), 241–257 (2007).
37. A. A. Sorokin, A. B. Kotov, E. B. Sal'nikova, A. P. Sorokin, S. Z. Yakovleva, Yu. V. Plotkina, and B. M. Gorokhovskii, "The Early Paleozoic age of granitoides of the Kiviliyskii complex of the Bureya Terrane (eastern flank of the Central Asian Fold Belt)," Dokl. Earth Sci. **440** (1), 1253–1257 (2011).
38. A. A. Sorokin, Yu. V. Smirnov, Yu. N. Smirnova, and N. M. Kudryashov, "First data on age of metarhyolites from the Turan Group of the Bureya Terrane, eastern part of the Central Asian Foldbelt," Dokl. Earth Sci. **439** (1), 944–948 (2011).
39. A. A. Sorokin, Yu. V. Smirnov, A. B. Kotov, and V. P. Kovach, "Age and source of terrigenous rocks of the Turan Group of the Bureya Terrane of the eastern part of the Central Asian Foldbelt: results of geochemical (Sm–Nd) and geochronological (U–Pb LA–ICP–MS) studies," Dokl. Earth Sci. **456** (2), 759–763 (2014).
40. A. A. Sorokin, N. M. Kudryashov, A. B. Kotov, and V. P. Kovach, " First evidence of Ediacaran magmatism in the geological history of the Mamyn terrane of the Central Asian Fold Belt," Russ. J. Pac. Geol. **9** (6), 399–410 (2015).
41. A. A. Sorokin, A. B. Kotov, Yu. N. Smirnova, E. B. Sal'nikova, Yu. V. Plotkina, S. Z. Yakovleva, "Age of terrigenous deposits of the Khingan Group in the Lesser Khingan terrane in the eastern part of the Central Asian Fold Belt," Dokl. Earth Sci. **471** (1), 1126–1130 (2016).
42. A. A. Sorokin, R. O. Ovchinnikov, N. M. Kudryashov, A. B. Kotov, and V. P. Kovach, "Two stages of Neoproterozoic magmatism in the evolution of the Bureya continental massif of the Central Asian Fold Belt," Russ. Geol. Geophys. **58** (10), 1171–1187 (2017).
43. A. I. Khanchuk, V. V. Ratkin, M. D. Ryazantseva, V. V. Golozubov, and N. G. Gonokhova, *Geology and Mineral Resources of Primorye* (Dal'nauka, Vladivostok, 1995) [in Russian].

44. A. I. Khanchuk, G. M. Vovna, V. I. Kiselev, M. A. Mishkin, and S. N. Lavrik, "First results of zircon LA-ICP-MS U–Pb dating of the rocks from the granulite complex of Khanka Massif in the Primorye region," Dokl. Earth Sci. **434** (1), 1164–1167 (2010).

45. A. I. Khanchuk, V. G. Sakhno, and A. A. Alenicheva, "First SHRIMP U–Pb zircon dating of magmatic complexes in the southwestern Primor'e region," Dokl. Earth Sci. **431** (2), 424–428 (2010).

46. A. I. Khanchuk, V. G. Nevstruev, N. V. Berdnikov, and V. P. Nechaev, "Petrochemical characteristics of carbonaceous shales in the eastern Bureya massif and their precious-metal mineralization," Russ. Geol. Geophys. **54** (6), 627–636 (2013).

47. A. I. Khanchuk, A. V. Grebennikov, and V. V. Ivanov, "Albian–Cenomanian orogenic belt and igneous province of Pacific Asia," Russ. J. Pac. Geol. **13** (3), 187–219 (2019).

48. S. A. Shcheka, *Mafic–Ultramafic Intrusions and Inclusions in the Volcanic Rocks of Far East* (Nauka, Moscow, 1983) [in Russian].

49. J. H. Bi, W. C. Ge, H. Yang, Z. H. Wang, W. L. Xu, J. H. Yang, D. H. Xing, and H. J. Chen, "Geochronology and geochemistry of Late Carboniferous–Middle Permian I- and A-type granites and gabbro-diorites in the eastern Jiamusi Massif, NE China: Implications for petrogenesis and tectonic setting," Lithos **266–267**, 213–232 (2016).

50. J. H. Bi, W. C. Ge, H. Yang, G. C. Zhao, J. J. Yu, Y. L. Zhang, Z. H. Wang, and D. X. Tian, "Petrogenesis and tectonic implications of Early Paleozoic granitic magmatism in the Jiamusi Massif, NE China: geochronological, geochemical and Hf isotopic evidence," J. Asian Earth Sci **96**, 308–331 (2014).

51. H. H. Cao, W. L. Xu, F. P. Pei, and X. Z. Zhang, "Permian Tectonic Evolution in Southwestern Khanka Massif: Evidence from Zircon U-Pb Chronology, Hf Isotope and geochemistry of gabbro and diorite," Acta Geol. Sin **85**, 1390–1402 (2011).

52. C. Chen, Y. S. Ren, H. L. Zhao, X. T. Zou, Q. Yang, and Z. C. Hu, "Permian age of the Wudaogou Group in eastern Yanbian: Detrital Zircon U-Pb constraints on the closure of the Palaeo-Asian Ocean in Northeast China," Int. Geol. Rev. **56**, 1754–1768 (2014).

53. M. Ehiro, "Origins and drift histories of some microcontinents distributed in the eastern margin of Asian Continent," Earth Sci. (Chikyu Kagaku) **55** (2), 71–81 (2001).

54. P. R. Eizenhofer and G. Zhao, "Solonker suture in E Asia and its bearing on the final closure of the eastern segment of the Palaeo-Asian Ocean," Earth Sci. Rev. **186**, 153–172 (2018).

55. Z. Q. Feng, W. M. Li, Y. J. Liu, W. Jin, Q. B. Wen, B. Q. Liu, J. P. Zhou, T. A. Zhang, and X. Y. Li, "Early Carboniferous tectonic evolution of the northern Heihe–Nenjiang–Hegenshan suture zone, NE China: Constraints from the mylonitized Nenjiang rhyolites and the Moguqi gabbros," Geol. J. **53** (3), 1005–1021 (2017).

56. Z. Q. Feng, Y. J. Liu, P. Wu, W. Jin, W. M. Li, Q. B. Wen, Y. L. Zhao, and J. P. Zhou, "Silurian magmatism on the eastern margin of the Erguna Block, NE China: Evolution of the northern Great Xing'An Range," Gondwana Res. **61**, 46–62 (2018).

57. M. H. Ge, L. Li, T. Wang, J. J. Zhang, Y. Tong, L. Guo, K. Liu, L. Feng, P. Song, and J. G. Yuan, "Hf isotopic mapping of the Paleozoic–Mesozoic granitoids from the Jiamusi and Songnen blocks, NE China: implications for their tectonic division and juvenile continental crustal growth," Lithos **386–387** (3), 106048 (2021).

58. V. V. Golozoubov, V. S. Markevich, and E. V. Bugdaeva, "Early Cretaceous changes of vegetation and environment in E. Asia," Palaegeogr., Palaeclimat., Palaeecol, No. **153**, 139–146 (1999).

59. W. L. Xu, Z. Wang, F. Wang, and J. P. Luan, "Geochronology and geochemistry of Late Devonian–Carboniferous igneous rocks in the Songnen–Zhangguangcai range massif, NE China: constraints on the Late Paleozoic tectonic evolution of the eastern Central Asian Orogenic Belt," Gondwana Res. **57**, 119–132 (2018).

60. S. J. Han, Y. C. Yang, J. W. Bo, G. B. Zhang, V. G. Khomich, Y. W. Huang, Y. B. Yang, and X. Y. Wang, "Late Neoarchean magmatic record of the Jiamusi–Khanka block, northeast China new clues from amphibolite zircon U-Pb geochronology and Lu-Hf Isotopes," Geol. J. **55** (5), 3401–3415 (2019).

61. X. L. Hu, S. Z. Yao, C. Y. Tan, G. P. Zeng, Z. J. Ding, and M. C. He, "Early Paleozoic geodynamic evolution of the eastern Central Asian Orogenic Belt: insights from granitoids in the Xing'An and Songnen blocks," Geosci. Front. **11**, 1975–1992 (2020).

62. Y. Isozaki, H. Nakahata, Y. D. Zakharov, A. V. Popov, S. Sakata, and T. Hirata, "Greater South China extended to the Khanka Block: detrital zircon geochronology of Middle–Upper Paleozoic sandstones in Primorye, Far East Russia," J. Asian Earth Sci **145**, 565–575 (2017).

63. C. L. Kirkland, R. H. Smithies, R. J. M. Taylor, N. Evans, and B. McDonald, "Zircon Th/U ratios in magmatic environs," Lithos **212**, 397–414 (2015).

64. J. Y. Li, "Permian geodynamic setting of NE China and adjacent regions: closure of the Paleo-Asian Ocean and subduction of the Paleo-Pacific plate," J. Asian Earth Sci. **26** ((3)), 207–224 (2006).

65. B. Liu, J. F. Chen, B. F. D. Han, J. L. Liu, and J. W. Li, "Geochronological and geochemical evidence for a Late Ordovician t Silurian arc–back-arc system in the northern Great Xing'An Range, NE China," Geosci. Front. **12** (1), 131–145 (2021).

66. Y. Liu, W. Li, Y. Ma, Z. Feng, Q. Guan, S. Li, Z. Chen, C. Liang, and Q. Wen, "An orocline in the eastern Central Asian Orogenic Belt," Earth Sci. Rev. **221**, 1–33 (2021).

67. J. P. Luan, F. Wang, W. L. Xu, W. C. Ge, A. A. Sorokin, Z. W. Wang, and P. Guo, "Provenance, age, and tectonic implications of Neoproterozoic strata in the Jiamusi Massif: Evidence from U-Pb ages and Hf isotope compositions of detrital and magmatic zircons," Precambrian Res. **297**, 19–32 (2017).

68. J. P. Luan, W. L. Xu, F. Wang, Z. W. Wang, and P. Guo, "Age and geochemistry of Neoproterozoic granitoids in the Songnen–Zhangguangcai Range

massif, NE China: Petrogenesis and tectonic implications," J. Asian Earth Sci **148**, 265–276 (2017).

69. J. P. Luan, J. J. Yu, J. L. Yu, Y. C. Cui, and W. L. Xu, "Early Neoproterozoic magmatism and the associated metamorphism in the Songnen Massif, NE China: petrogenesis and tectonic implications," Precambrian Res. **328**, 250–268 (2019).
70. X. H. Ma, C. J. Chen, J. X. Zhao, S. L. Qiao, and Z. H. Zhou, "Late Permian intermediate and felsic intrusions in the eastern Central Asian Orogenic Belt: final-stage magmatic record of Paleo-Asian oceanic subduction?," Lithos **326–327**, 265–278 (2019).
71. A. A. Sorokin, W. L. Xu, H. Yang, V. P. Kovach, A. B. Kotov, and Yu. V. Plotkina, "Provenance and tectonic implications of Cambrian sedimentary rocks in the Bureya Massif, Central Asian Orogenic Belt," J. Asian Earth Sci **172**, 393–408 (2019).
72. R. O. Ovchinnikov, A. A. Sorokin, N. M. Kudryashov, V. P. Kovach, Yu. V. Plotkina, and T. M. Skovitina, "Age of the Early Paleozoic granitoid magmatism in the central part of the Bureya continental massif, Central Asian Fold Belt," Geodynamics & Tectonophysics **11** ((1)), 89–106 (2020).
73. R. O. Ovchinnikov, A. A. Sorokin, and N. M. Kydryashov, "Early Paleozoic magmatic events in the Bureya continental massif, Central Asian Orogenic Belt: Timing and tectonic significance," Lithos **396–397**, 106237 (2021).
74. L. M. Parfenov, G. Badarch, N. A. Berzin, A. I. Khanchuk, M. I. Kuzmin, W. J. Nokleberg, A. V. Prokopiev, M. Ogasawara, and H. Yan, "Summary of northeast Asia geodynamics and tectonics," Stephan Mueller Spec. Publ., Ser. 4, 11–33 (2009).
75. N. G. Rizvanova, A. A. Alenicheva, S. G. Skublov, S. A. Sergeev, and D. A. Lykhin, "Early Ordovician age of fluorite–rare-metal deposits at the Voznesensky ore district (Russia): evidence from zircon and cassiterite U-Pb and fluorite Sm-Nd dating results," Minerals **11**, 1–2 (2021).
76. T. Sang, F. Pei, W. Xu, Z. Wang, J. Jiao, J. Wei, Y. Wang, "Detrital zircon U-Pb geochronology of Xilin Group: Constraints for the Early Paleozoic tectonic evolution of the Songliao Massif," Acta Geol. Sinica (2021). https://doi.org/10.1111/1755-6724.14684
77. S. Schuth, V. I. Gornyy, J. Berndt, S. S. Shevchenko, S. A. Sergeev, A. F. Karpuzov, and T. Mansfeldt, "Early Proterozoic U-Pb zircon ages from basement gneiss at the Solovetsky Archipelago, White Sea, Russia," Int. J. Geosci. **3** (2), 289–296 (2012).
78. A. M. C. Sengor and B. A. Natal'in, "Paleotectonics of Asia: Fragments of a synthesis," *The Tectonic Evolution of Asia*, Ed. by A. Yin and M. Harrison (Cambridge Univ. Press, Cambridge, 1996), pp. 486–614.
79. X. Shen, Q. Du, Z. Han, Z. Song, C. Han, and W. Zhong, "Constraints of zircon U-Pb-Hf isotopes from Late Permian–Middle Triassic flora-bearing strata in the Yanbian area (NE China) on a scissorlike closure model of the Paleo-Asian Ocean," J. Asian Earth Sci. **183** (2019).
80. A. A. Sorokin, N. M. Kudryashov, A. B. Kotov, and V. P. Kovach, "Age and tectonic setting of the Early Paleozoic magmatism of the Mamyn Terrane, Central Asian Orogenic Belt, Russia," J. Asian Earth Sci **144**, 22–39 (2017).
81. A. A. Sorokin, R. O. Ovchinnikov, W. L. Xu, V. P. Kovach, H. Yang, A. B. Kotov, V. A. Ponomarchuk, A. V. Travin, and Yu. V. Plotkina, "Ages and nature of the protolith of the Tulovchikha metamorphic complex in the Bureya Massif, Central Asian Orogenic Belt, Russia: Evidence from U-Th-Pb, Lu-Hf, Sm-Nd, and $^{40}Ar/^{39}Ar$ Data," Lithos **332–333**, 340–354 (2019).
82. A. A. Sorokin, V. A. Zaika, V. P. Kovach, A. B. Kotov, W. Xu, "Timing of closure of the eastern Mongol–Okhotsk Ocean: Constraints from U-Pb and Hf isotopic data of detrital zircons from metasediments along the Dzhagdy transect," Gondwana Res. **81**, 58–78 (2020).
83. A. A. Sorokin, V. A. Zaika, and N. M. Kudryashov, "Timing of formation and tectonic setting of Paleozoic granitoids in the eastern Mongol-Okhotsk Belt: Constraints from geochemical, U-Pb, and Hf isotope data," Lithos **388–389**, 340–354 (2021).
84. K. Tang, Y. Wang, G. He, and J. Shao, "Continetal-margin structure of northeast China and its adjacent areas," Acta Geol. Sinica **69**, 16 (1995).
85. Yu. Tsutsumi, K. Yokoyama, S. A. Kasatkin, and V. V. Golozoubov, "Age of igneous rocks in southern part of Primorye, Far East Russia," Memoirs of the National Museum of Nature and Science: Geological Research around and the Sea of Japan, No. 51, 71–78 (2016).
86. F. Wang, W. L. Xu, E. Meng, H. H. Cao, and F. H. Gao, "Early Paleozoic Amalgamation of the Songnen-Zhangguangcai Range and Jiamusi Massifs in the eastern segment of the Central Asian Orogenic Belt: Geochronological and geochemical evidence from granitoids and rhyolites," J. Asian Earth Sci **49**, 234–248 (2012).
87. F. Wang, W. L. Xu, F. H. Gao, H. H. Zhang, F. P. Pei, and L. Zhao, "Precambrian terrane within the Songnen–Zhangguangcai Range massif, NE China: Evidence from U-Pb ages of detrital zircons from the Dongfengshan and Tadong groups," Gondwana Res **26**, 402–413 (2014).
88. F. Wang, K. C. Xing, W. L. Xu, F. Z. Teng, Y. G. Xu, and D. B. Yang, "Permian ridge subduction in the easternmost Central Asian Orogenic Belt: Magmatic record using Sr–Nd–Pb–Hf–Mg isotopes," Lithos **384–385**, 1–11 (2021).
89. Z. W. Wang, W. L. Xu, F. P. Pei, F. Wang, P. Guo, F. Wang, and Y. Li, "Geochronology and geochemistry of Early Paleozoic igneous rocks from the Zhangguangcai Range, NE China: Constraints on tectonic evolution of the eastern Central Asian Orogenic Belt," Lithosphere **9** (5), 803–827 (2017).
90. S. A. Wilde, X. Z. Zhang, and F. Y. Wu, "Extension of a newly identified 500 Ma metamorphic terrane in north East China: further U-Pb SHRIMP dating of the Mashan Complex, Heilongjiang Province, China," Tectonophysics **328**, 115–130 (2000).
91. S. A. Wilde, F. Y. Wu, and G. Zhao, *The Khanka block, NE China, and Its significance for the evolution of the Central Asian Orogenic Belt and continental accre-*

tion, Geol. Soc. Spec. Publ. London **338**, 117–137 (2010).

92. F. Y. Wu, J. H. Yang, C. H. Lo, S. A. Wilde, D. Y. Sun, and B. M. Jahn, "The Heilongjiang Group: a Jurassic accretionary complex in the Jiamusi massif at the western pacific margin of northeastern China," Island Arc **16**, 156–172 (2007).
93. K. C. Xing, F. Wang, W. L. Xu, and F. H. Gao, "Tectonic affinity of the Khanka Massif in the easternmost Central Asian Orogenic Belt: Evidence from detrital zircon geochronology of Permian sedimentary rocks," Int. Geol. Rev. **62** (4), 428–445 (2020).
94. T. Xu, W. L. Xu, F. Wang, W. C. Ge, and A. A. Sorokin, "Geochronology and geochemistry of Early Paleozoic intrusive rocks from the Khanka Massif in the Russian Far East: Petrogenesis and tectonic implications," Lithos **300–301**, 105–120 (2018).
95. W. Ge, G. Zhao, Y. Dong, J. Bi, Z. Wang, J. Yu, and Y. Zhang, "Geochronology and geochemistry of Late Pan-African intrusive rocks in the Jiamusi–Khanka Block, NE China: Petrogenesis and geodynamic implications," Lithos **208–209**, 220–236 (2014).
96. H. Yang, W. C. Ge, G. C. Zhao, J. H. Bi, Z. H. Wang, Y. Dong, and W. L. Xu, "Zircon U-Pb ages and geochemistry of newly discovered Neoproterozoic orthogneisses in the Mishan Region, NE China: Constraints on the high-grade metamorphism and tectonic affinity of the Jiamusi–Khanka Block," Lithos **268–271**, 16–31 (2017).
97. W. C. Ge, J. H. Bi, Z. H. Wang, D. X. Tian, Y. Dong, and H. J. Chen, "The Neoproterozoic–Early Paleozoic evolution of the Jiamusi block, NE China and its east Gondwana connection: geochemical and zircon U-Pb-Hf isotopic constraints from the Mashan Complex," Gondwana Res. **54**, 102–121 (2018).
98. H. Yang, W. Xu, A. A. Sorokin, R. O. Ovchinnikov, and W. Ge, "Geochronology and geochemistry of Neoproterozoic magmatism in the Bureya Block, Russian Far East: Petrogenesis and implications for Rodinia reconstruction," Precambrian Res. **342**, 105676 (2020).
99. H. Yang, W. C. Ge, M. Santosh, Z. Ji, Y. Dong, Y. Jing, and H. R. Wu, "The role of continental fragments in the formation of intraoceanic arcs: Constraints from Sr–Nd–Hf–O isotopes of gabbro from the Jiamusi Block, NE China," Gondwana Res. **103**, 297–313 (2021).
100. S. Zhang, F. Wang, W. Xu, F. Gao, and J. Tang, "Tectonic history of the Huangsong tectonic terrains in the Khanka massif in the easternmost Central Asian Orogenic Belt: Constraints from detrital zircon U-Pb geochronology," Gondwana Res **99**, 149–162 (2021).
101. J. B. Zhou, S. A. Wilde, X. Z. Zhang, G. C. Zhao, C. Q. Zheng, Y. J. Wang, and X. H. Zhang, "The onset of Pacific margin accretion in NE China: Evidence from the Heilongjiang high-pressure metamorphic belt," Tectonophysics **478**, 230–246 (2009).
102. J. B. Zhou, S. A. Wilde, G. C. Zhao, X. Z. Zhang, C. Q. Zheng, H. Wang, and W. S. Zeng, "Pan-African metamorphic and magmatic rocks of the Khanka Massif, NE China: Further evidence regarding their affinity," Geol. Mag **147** (5), 737–749 (2010).
103. L. P. Zonenshain, M. I. Kuzmin, and L. M. Natapov, *Geology of the USSR: A Platetectonic Synthesis* (Am. Geophys. Union, Washington, 1990).

Recommended for publishing by A.A. Sorokin

Translated by M. Bogina